US 20080229832A1

(19) **United States**

(12) **Patent Application Publication**

Huang et al.

(10) **Pub. No.: US 2008/0229832 A1**

(43) **Pub. Date: Sep. 25, 2008**

(54) **AUTOMATIC TIME-OF-FLIGHT SELECTION FOR ULTRASOUND TOMOGRAPHY**

(75) Inventors: **Lianjie Huang**, Los Alamos, NM (US); **Cuiping Li**, Troy, MI (US)

Correspondence Address:
JOHN P. O'BANION
O'BANION & RITCHEY LLP
400 CAPITOL MALL SUITE 1550
SACRAMENTO, CA 95814 (US)

(73) Assignee: **LOS ALAMOS NATIONAL SECURITY**, Los Alamos, NM (US)

(21) Appl. No.: **12/033,789**

(22) Filed: **Feb. 19, 2008**

Related U.S. Application Data

(60) Provisional application No. 60/901,903, filed on Feb. 16, 2007.

Publication Classification

(51) **Int. Cl.**
G01N 29/00 (2006.01)
A61B 8/13 (2006.01)

(52) **U.S. Cl.** **73/620**; 73/597; 600/448

(57) **ABSTRACT**

Ultrasound sound-speed tomography requires accurate picks of time-of-flights (TOFs) of transmitted ultrasound signals, however, manual picking on large datasets is time-consuming. An improved automatic TOF picker is taught based on the Akaike Information Criterion (AIC) and multi-model inference (model averaging), based on the calculated AIC values, to improve the accuracy of TOF picks. The automatic TOF picker of the present invention can accurately pick TOFs in the presence of random noise with average absolute amplitude of up to 80% of the maximum absolute synthetic signal amplitude. The inventive method is applied to clinical ultrasound breast data, and compared with manual picks and amplitude threshold picking. Test results indicate that the inventive TOF picker is much less sensitive to data signal-to-noise ratios (SNRs), and performs more consistently for different datasets in relation to manual picking. The technique provides noticeably improved image reconstruction accuracy.

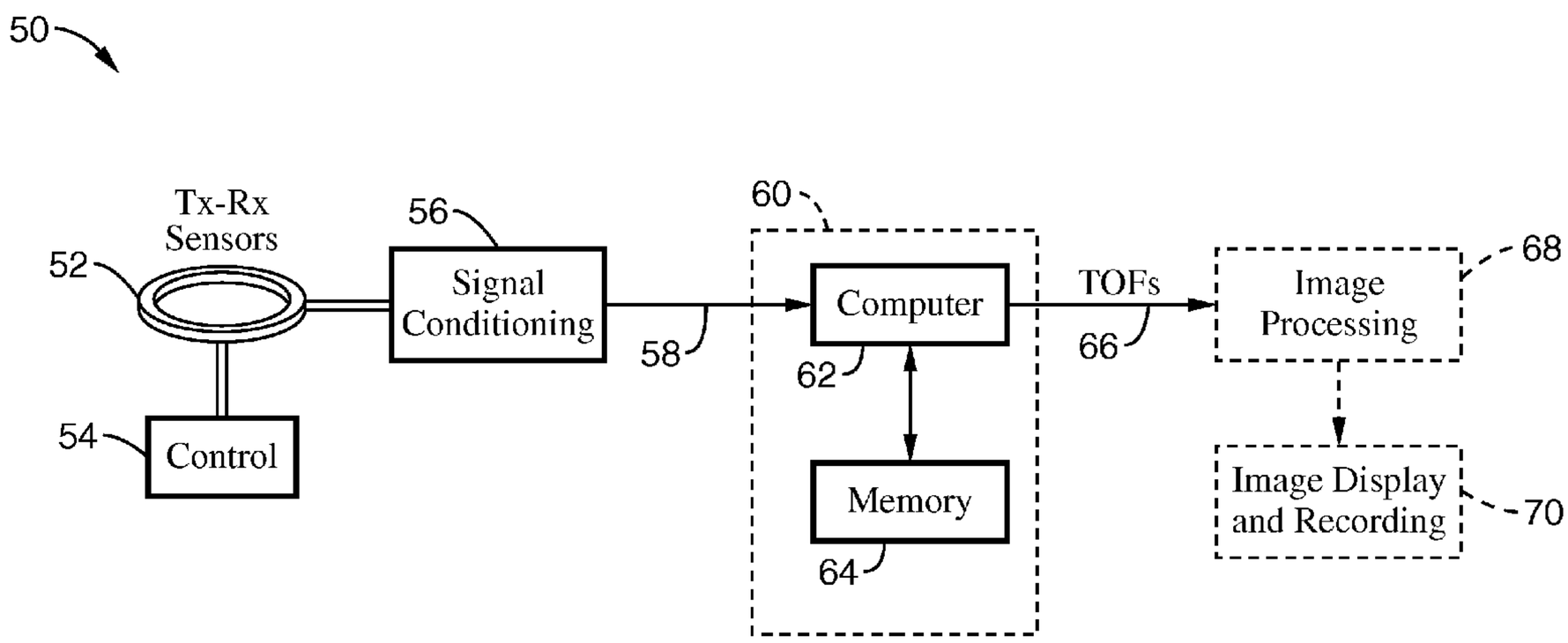

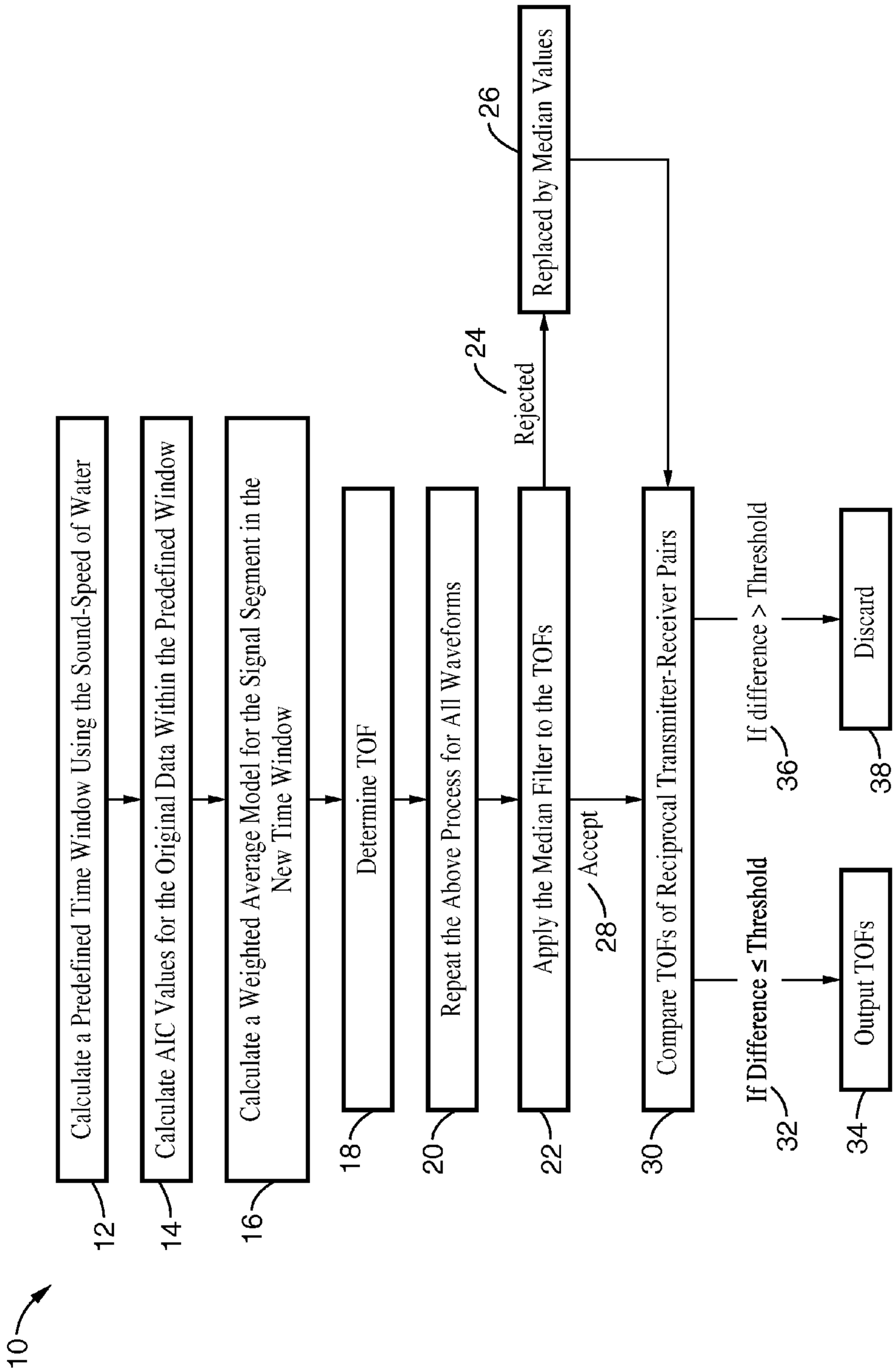
10
12
Calculate a Predefined Time Window Using the Sound-Speed of Water
14
Calculate AIC Values for the Original Data Within the Predefined Window
16
Calculate a Weighted Average Model for the Signal Segment in the New Time Window
18
Determine TOF
20
Repeat the Above Process for All Waveforms
22
Apply the Median Filter to the TOFs
24
Rejected
26
Replaced by Median Values
28
Accept
30
Compare TOFs of Reciprocal Transmitter-Receiver Pairs
32
If Difference ≤ Threshold
34
Output TOFs
36
If difference > Threshold
38
Discard

FIG. 1

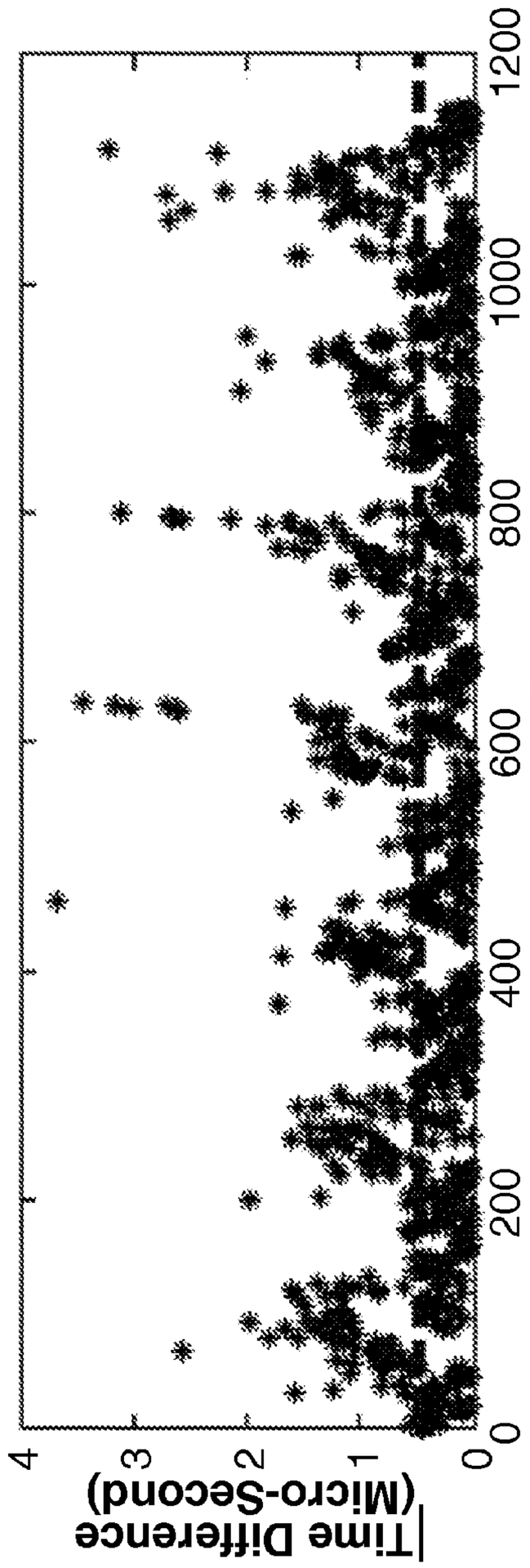
Time Difference
(Micro-Second)
0
1
2
3
4
200
400
600
800
1000
1200
Number of Data

FIG. 2A

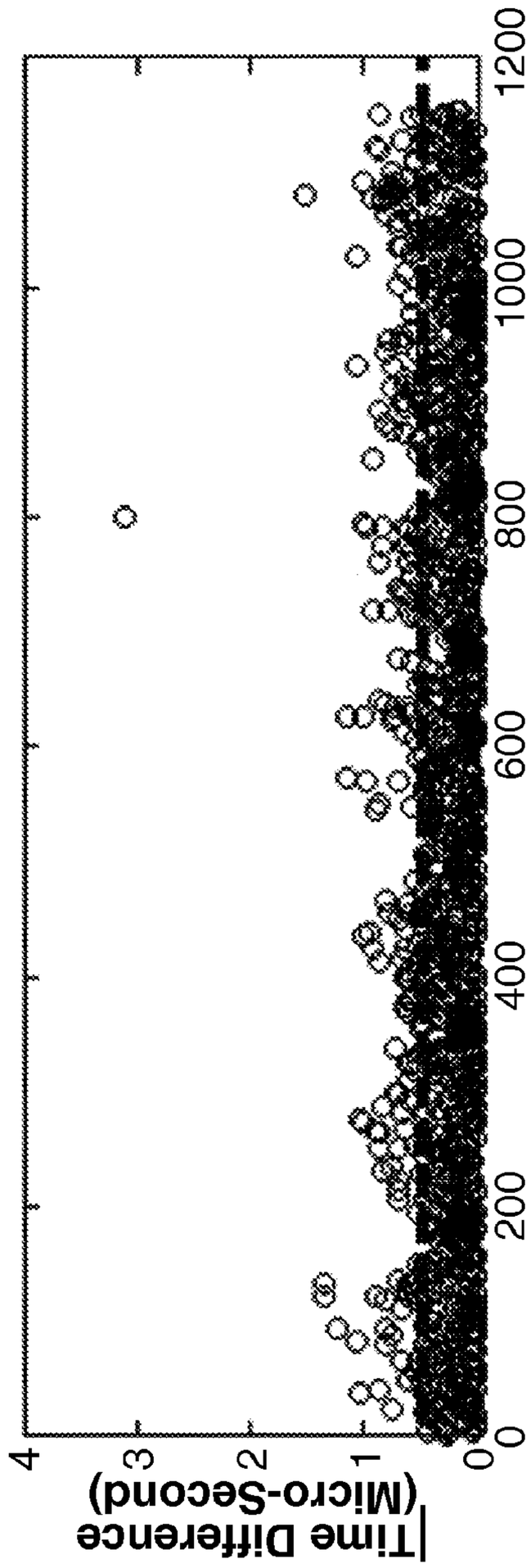
Time Difference
(Micro-Second)
0
1
2
3
4
200
400
600
800
1000
1200
Number of Data

FIG. 2B

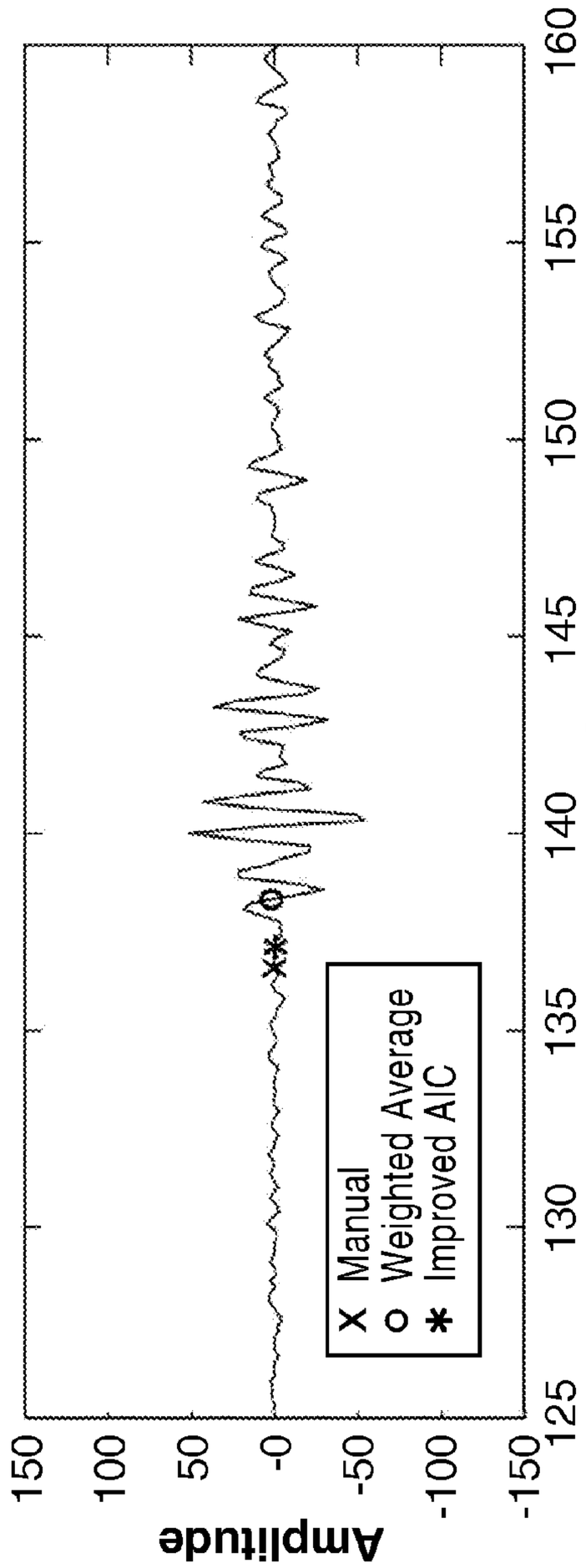
Amplitude
150
100
50
-0
-50
-100
-150
125
130
135
140
145
150
155
160
Micro-Second
X Manual
o Weighted Average
* Improved AIC

FIG. 3A

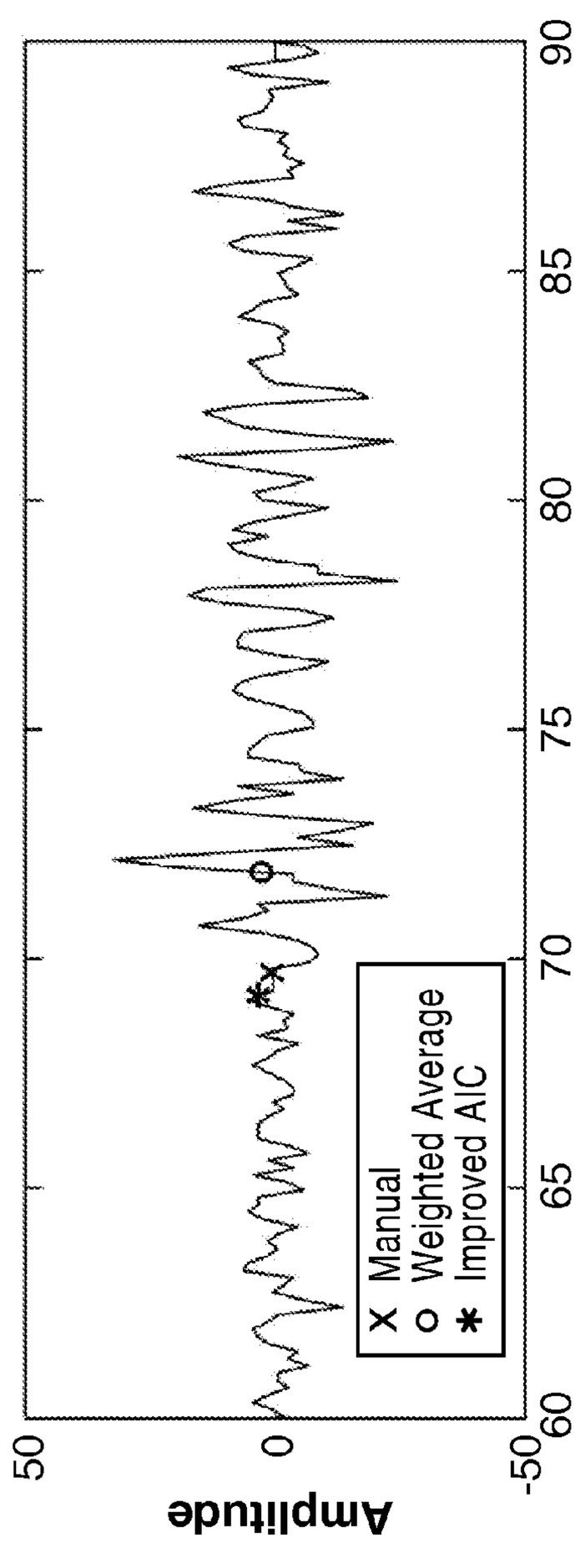
Amplitude
50
0
-50
60
65
70
75
80
85
90
Micro-Second
X Manual
o Weighted Average
* Improved AIC

FIG. 3B

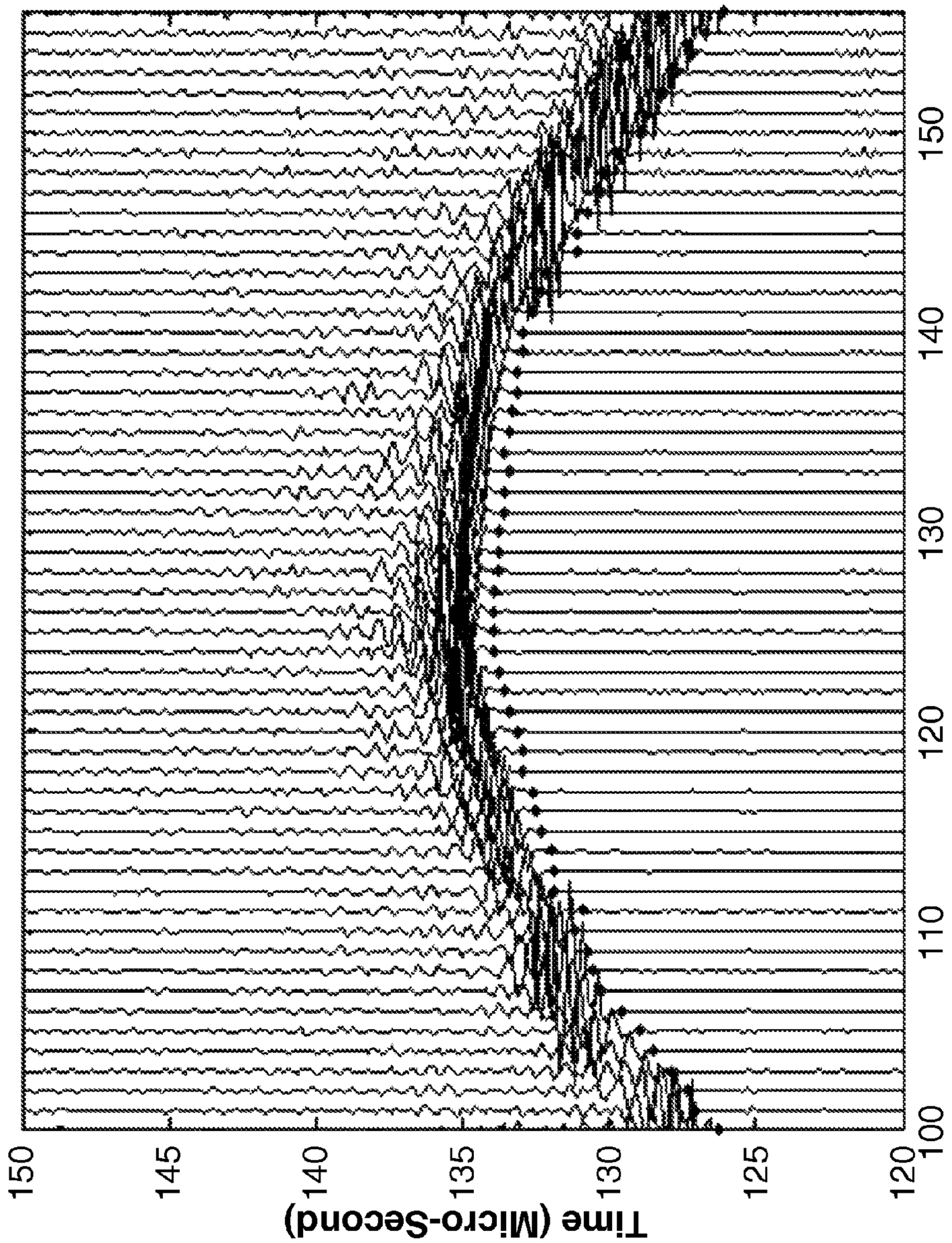
150
140
130
120
110
100
Receiver
150
145
140
135
130
125
120
Time (Micro-Second)

FIG. 4

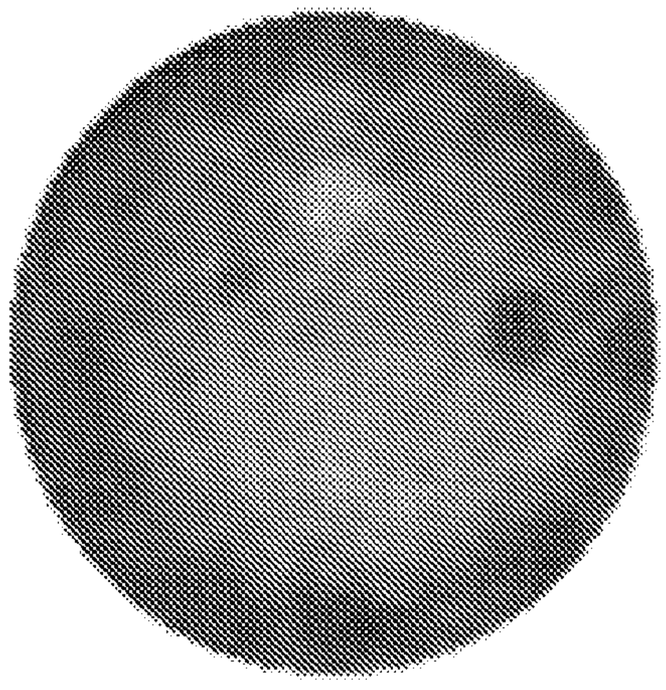

FIG. 5C

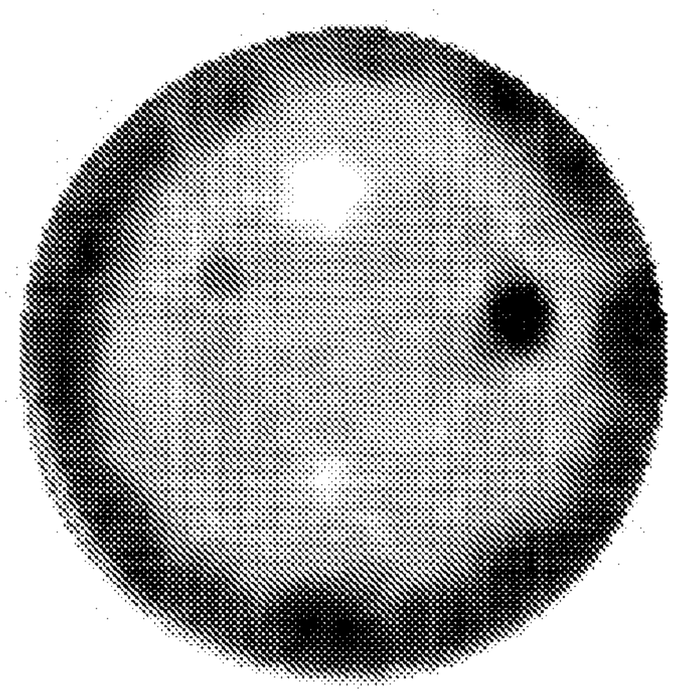

FIG. 5B

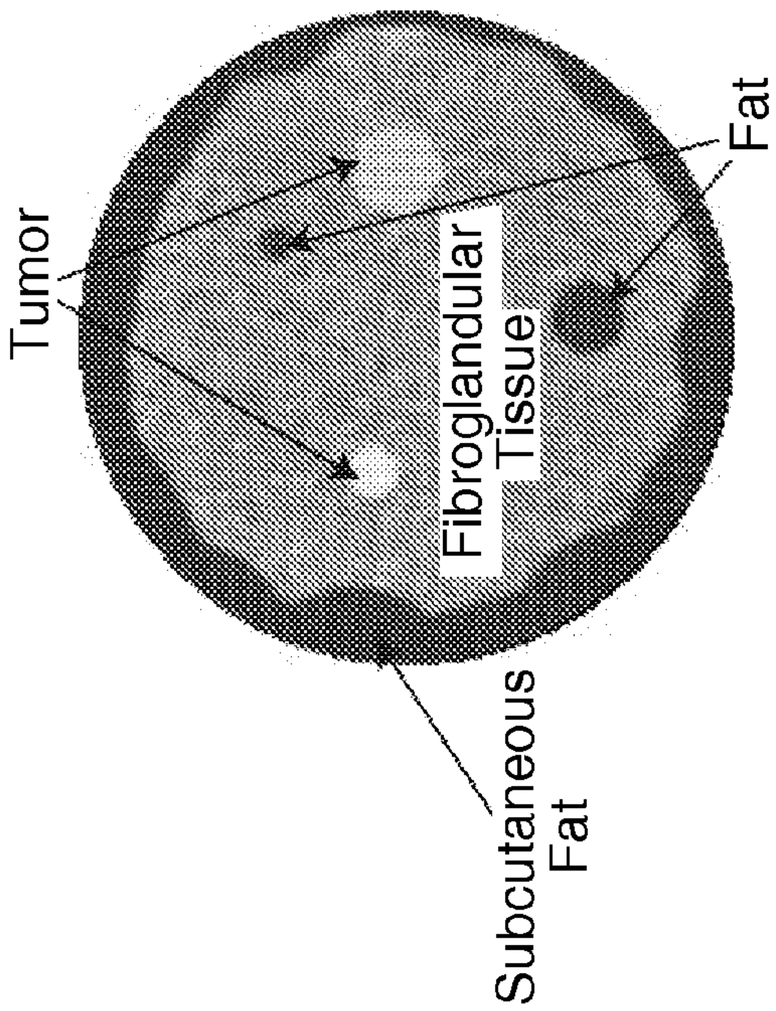

FIG. 5A

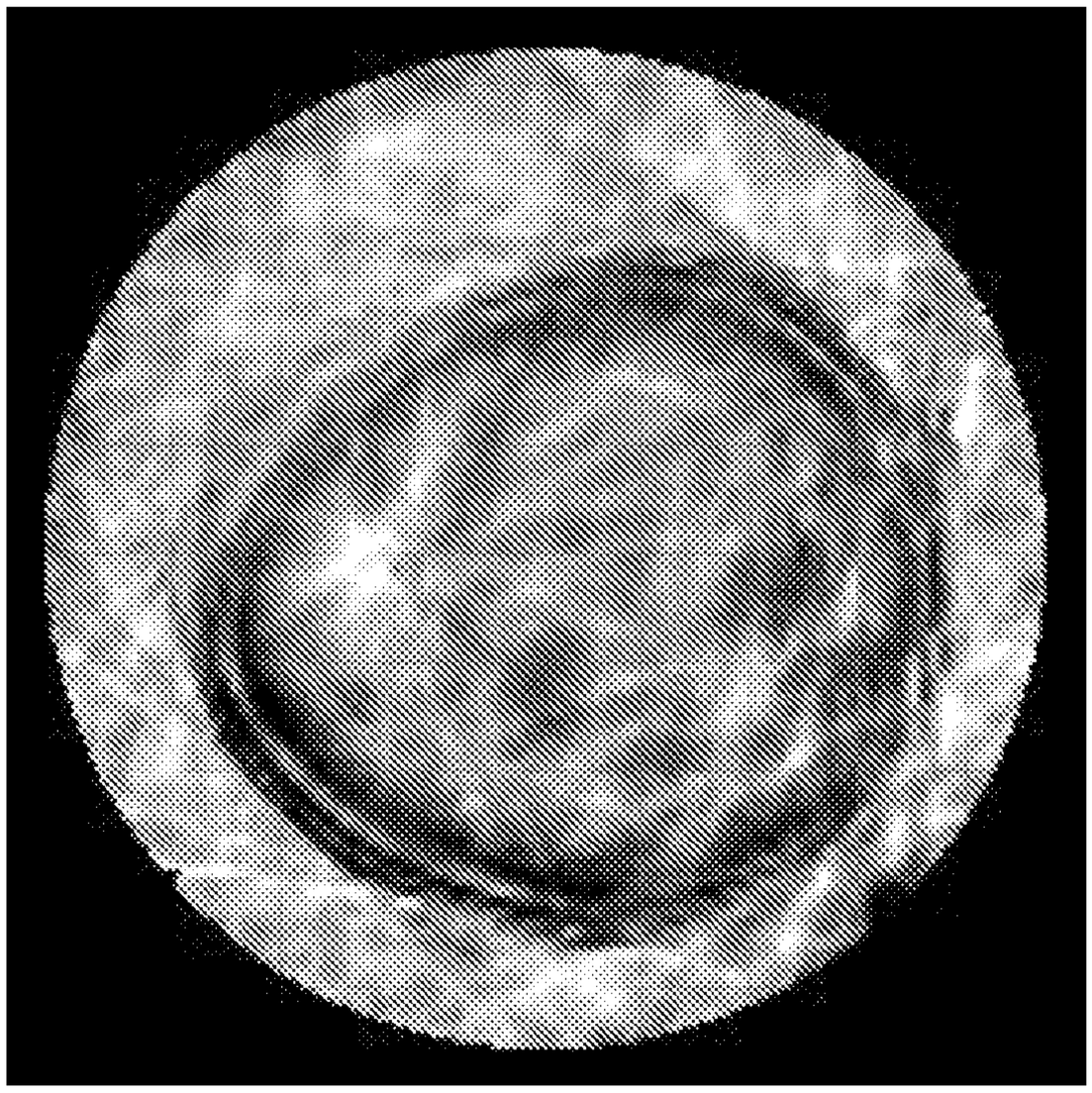

FIG. 6B

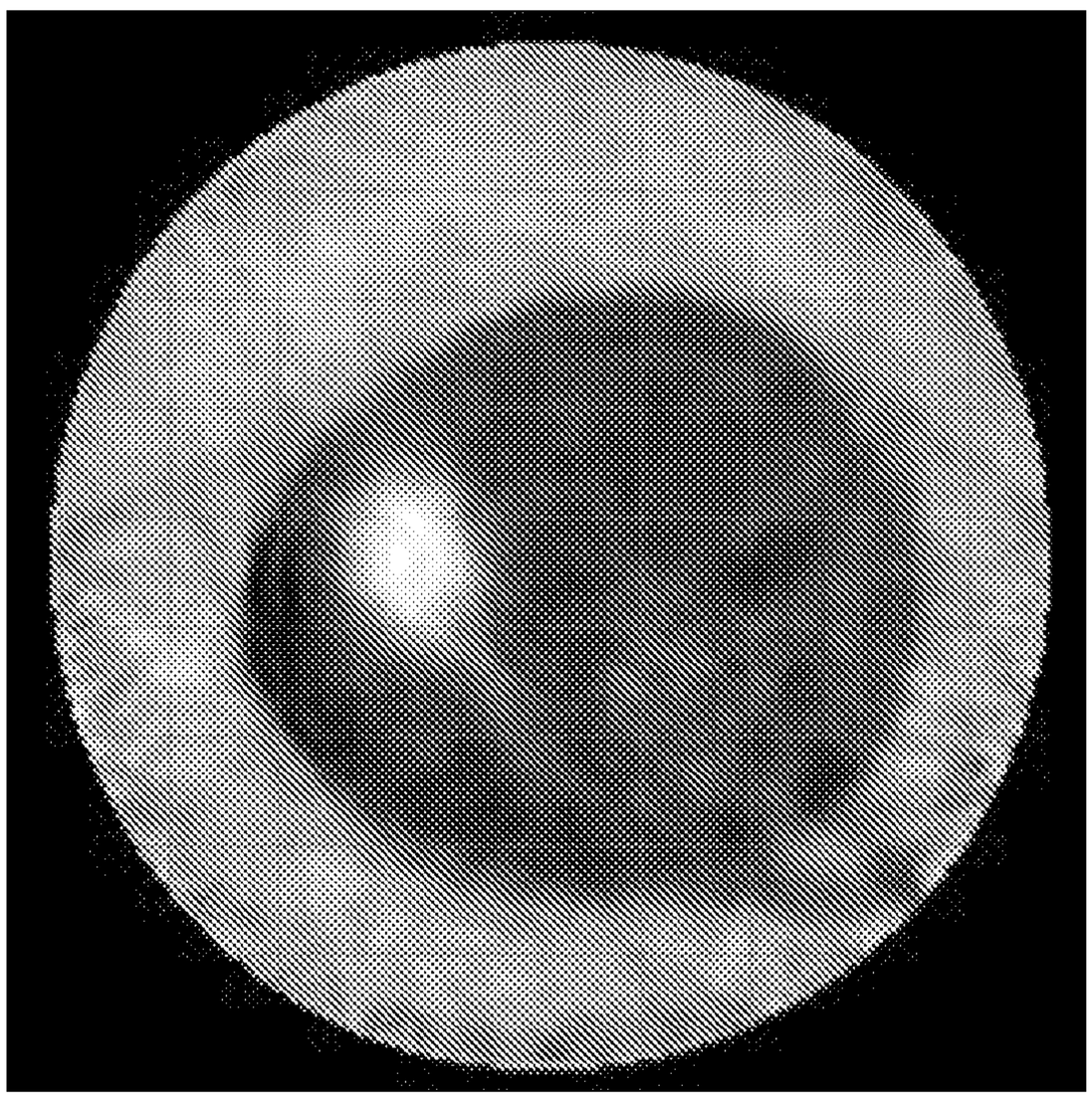

FIG. 6A

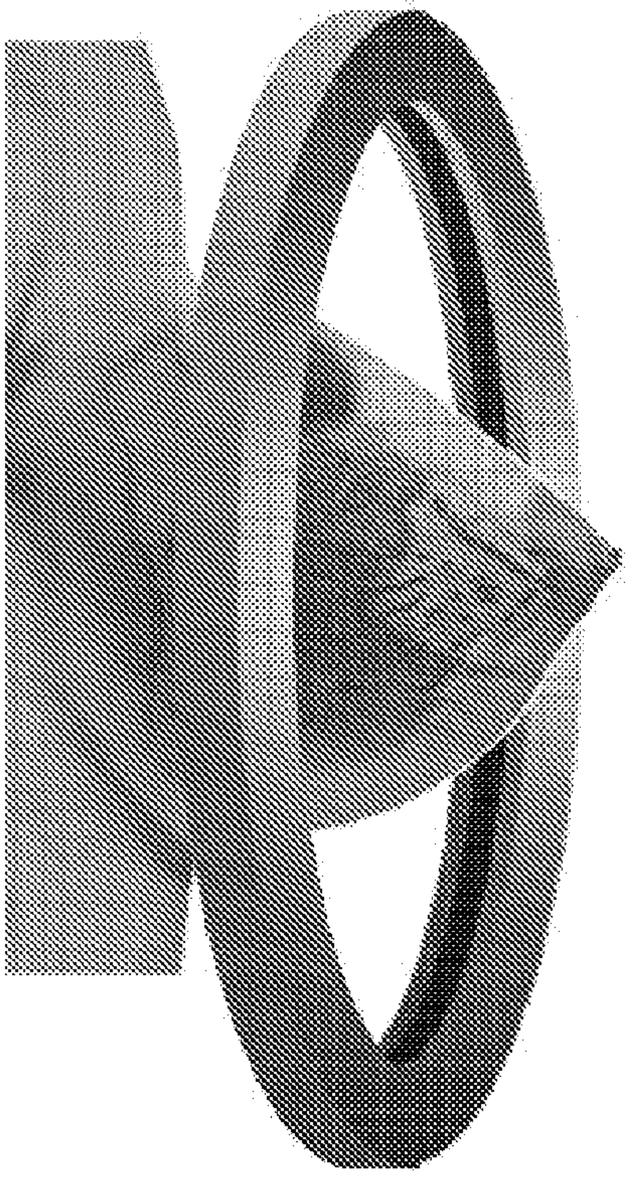

FIG. 7A

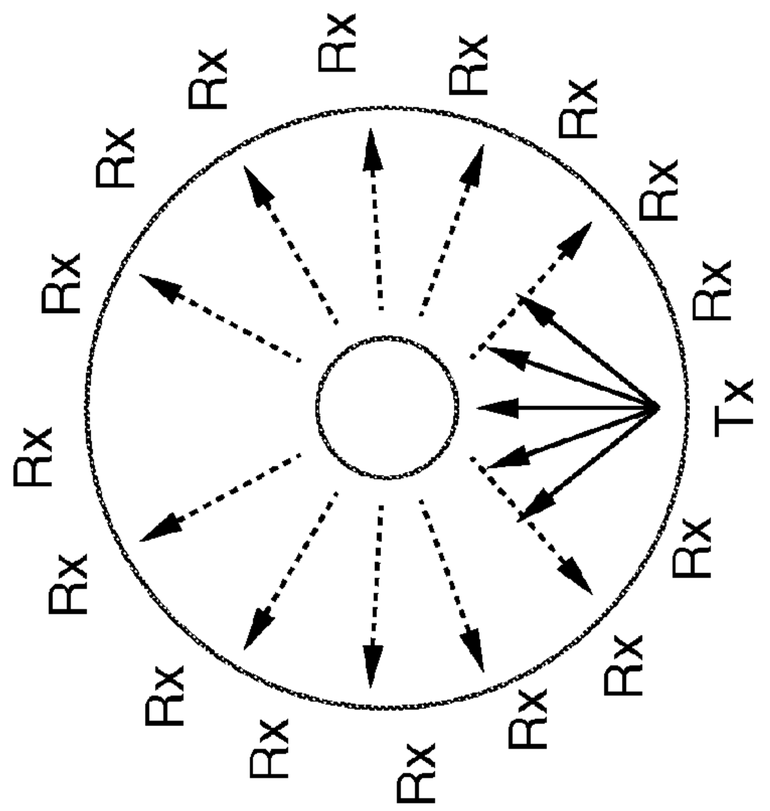

FIG. 7B

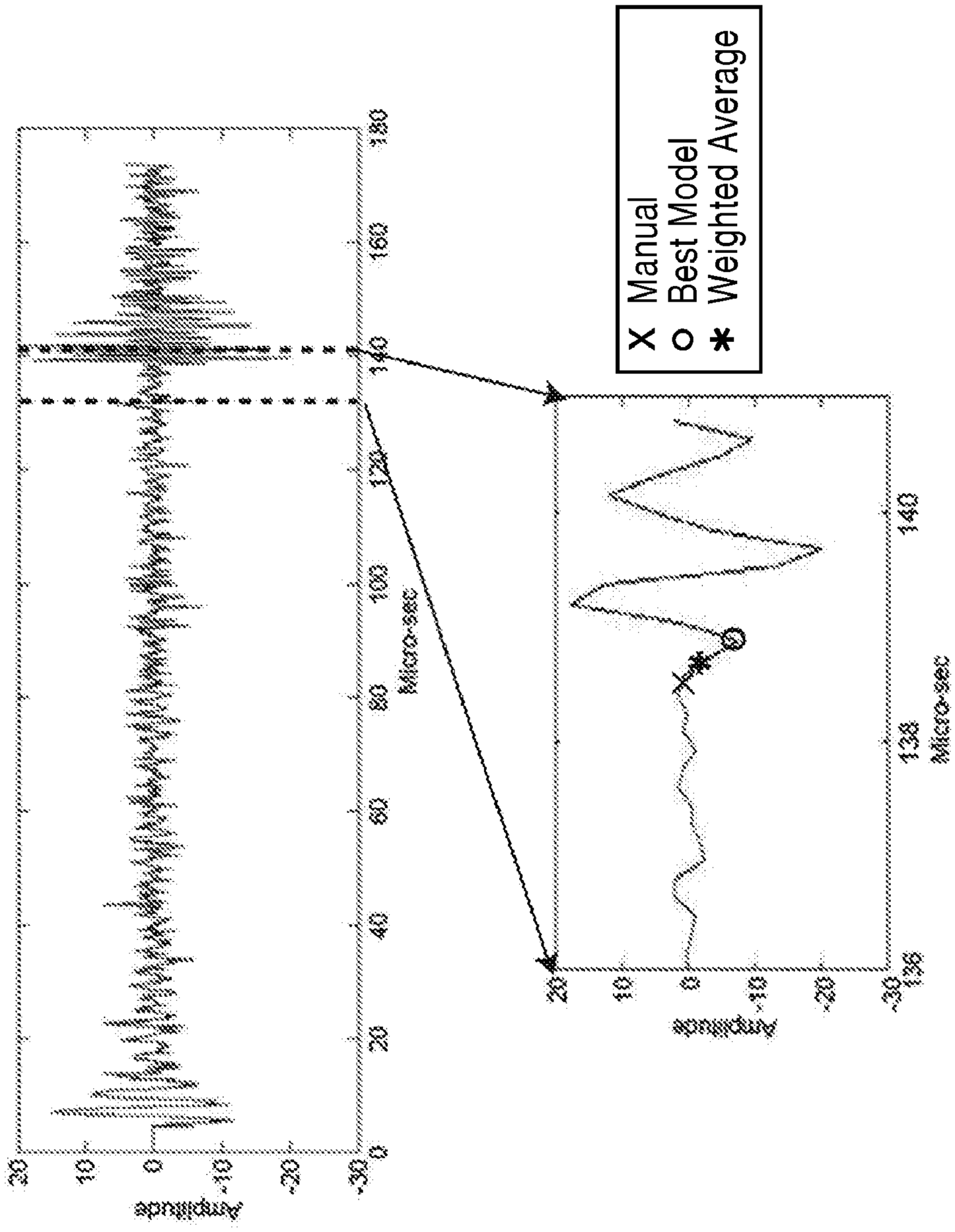
X Manual
O Best Model
* Weighted Average
Amplitude
Micro-sec
Amplitude
Micro-sec

FIG. 8

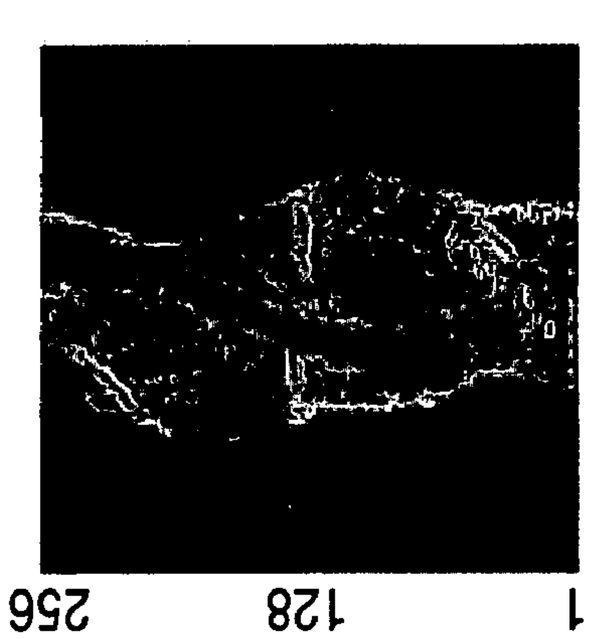

FIG. 9A

FIG. 9B

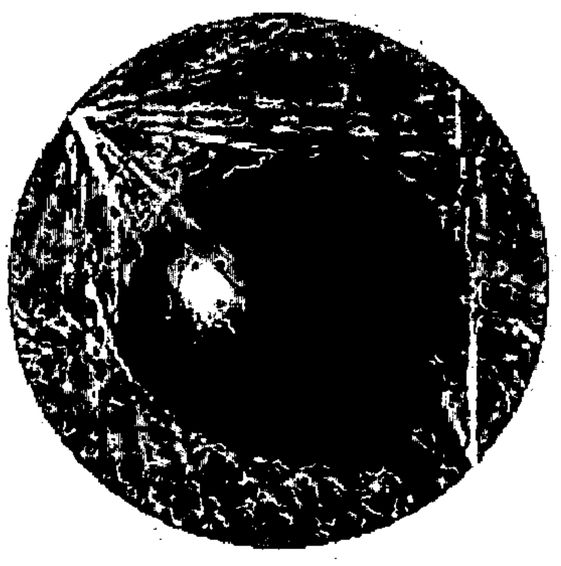

FIG. 9C

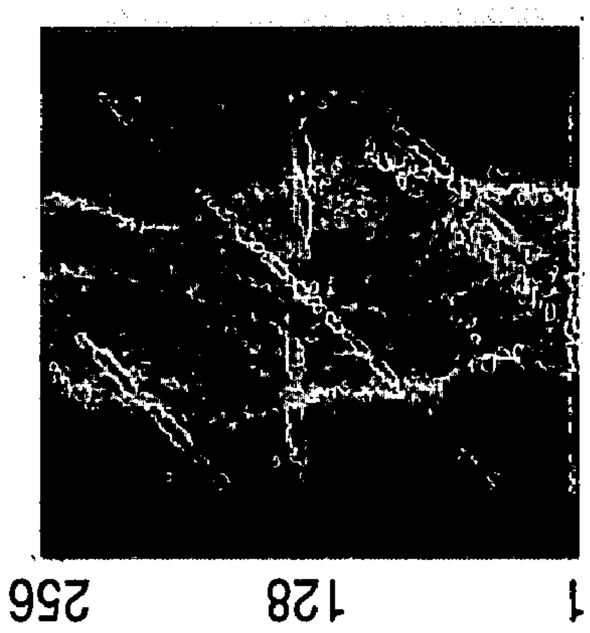

FIG. 9D

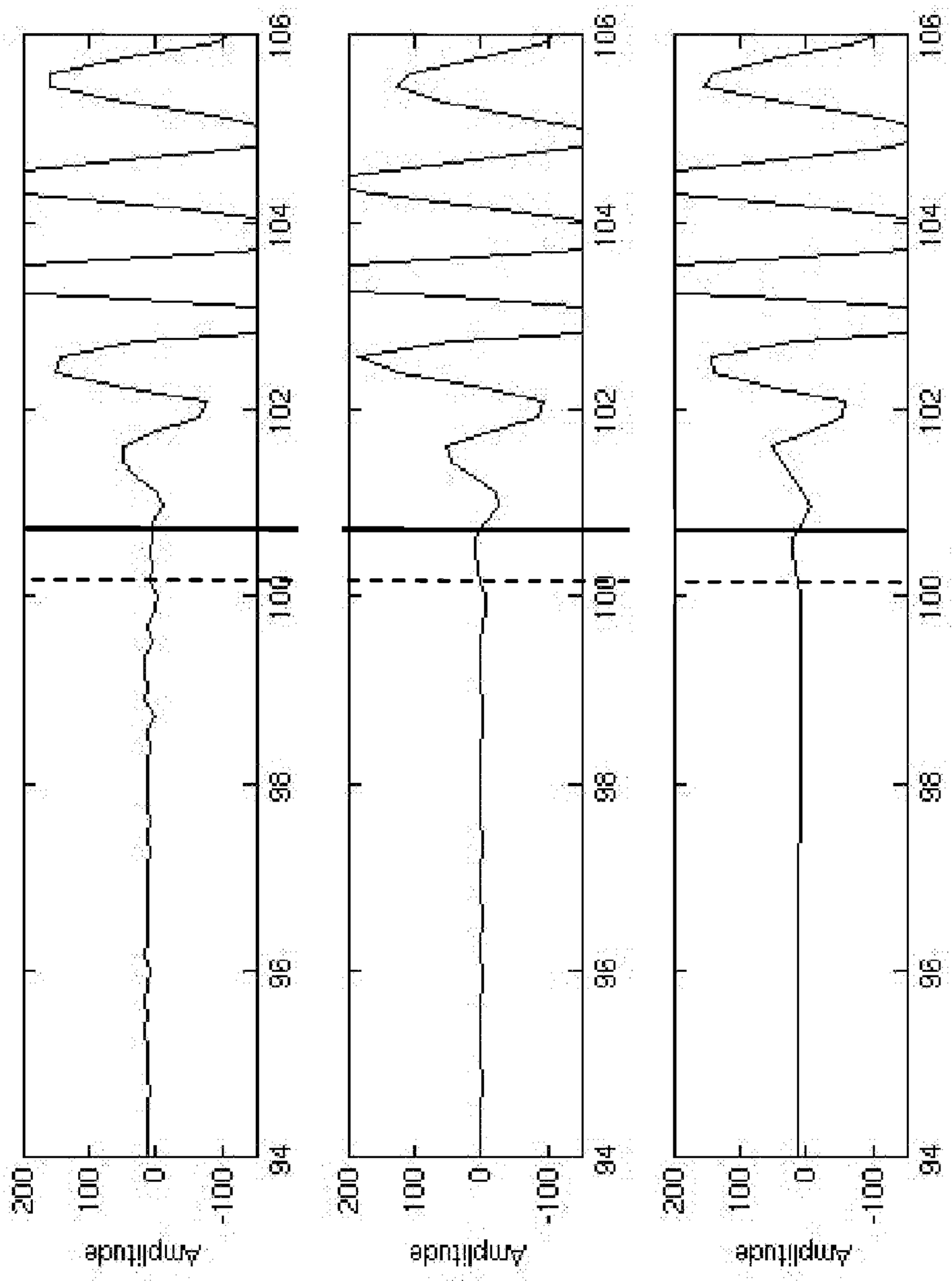

FIG. 10A

FIG. 10B

FIG. 10C

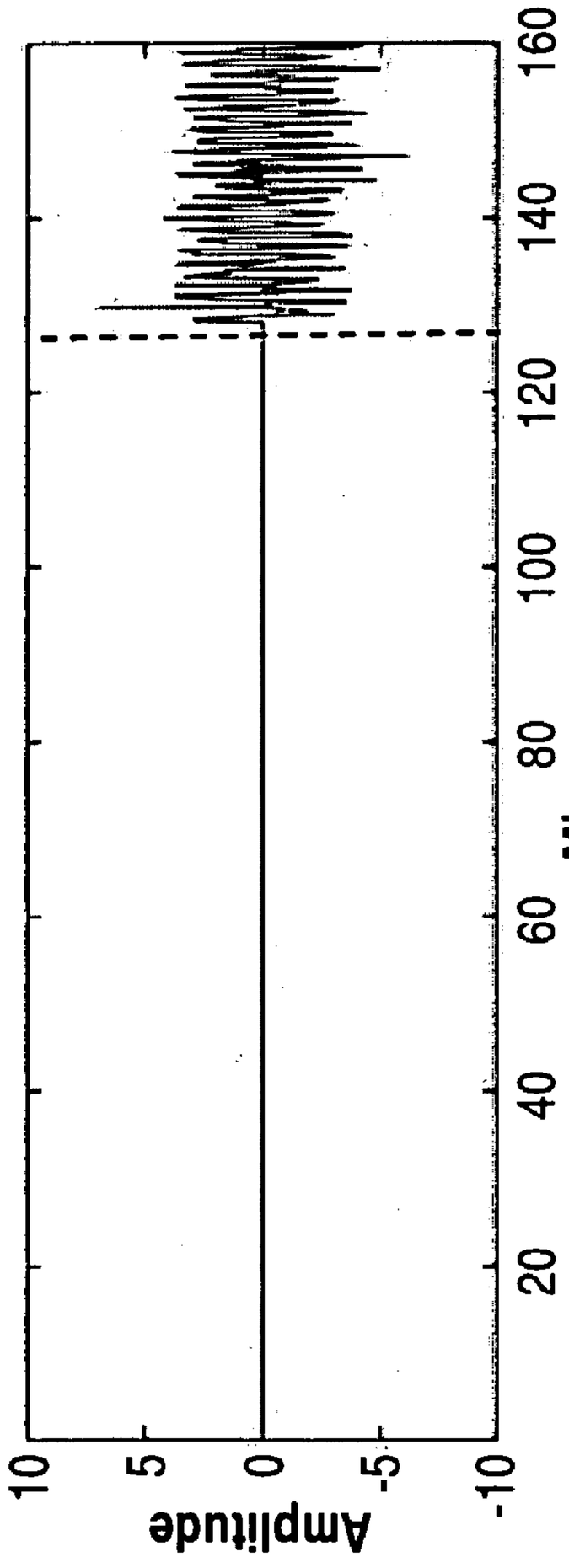

FIG. 11A

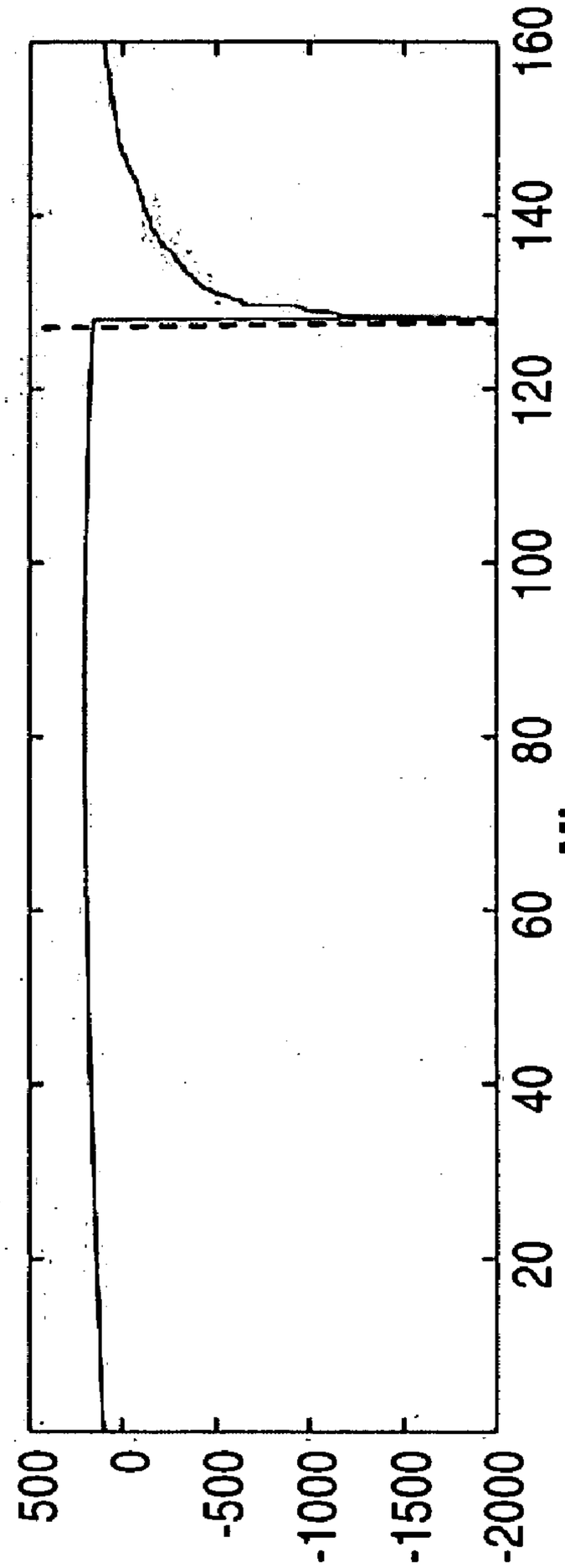

FIG. 11B

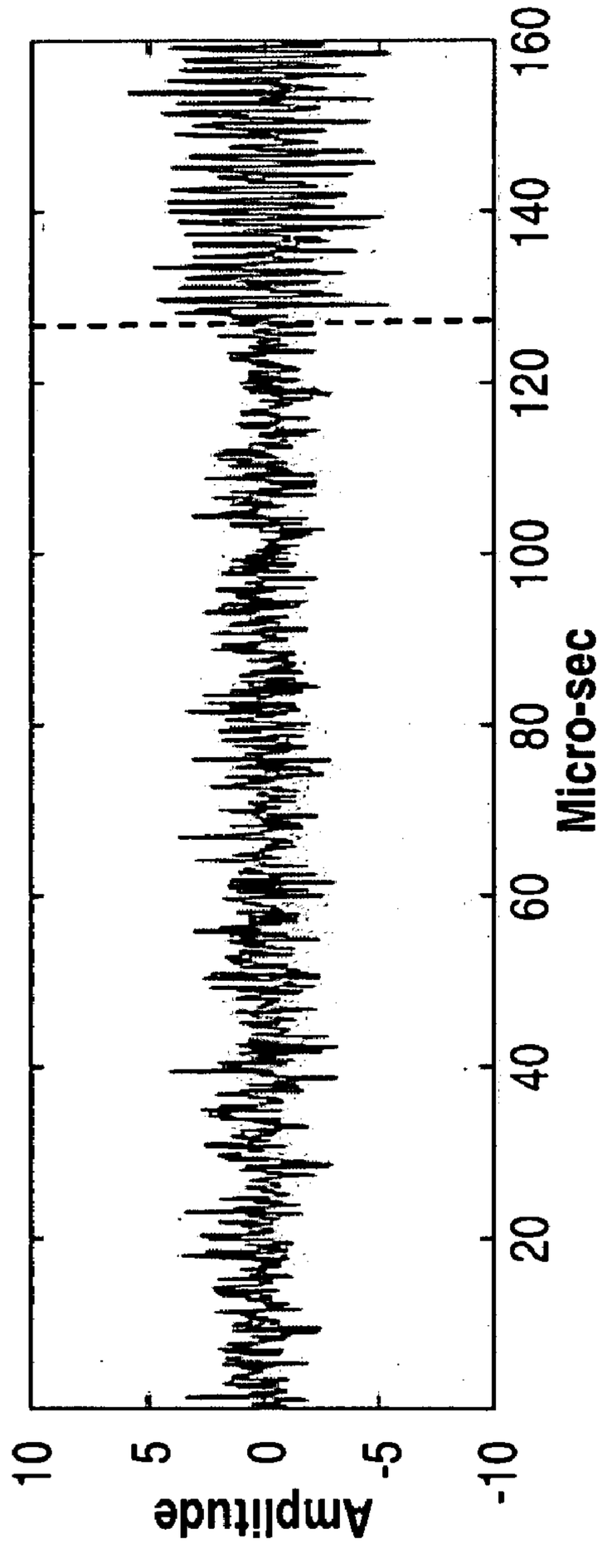

FIG. 12A

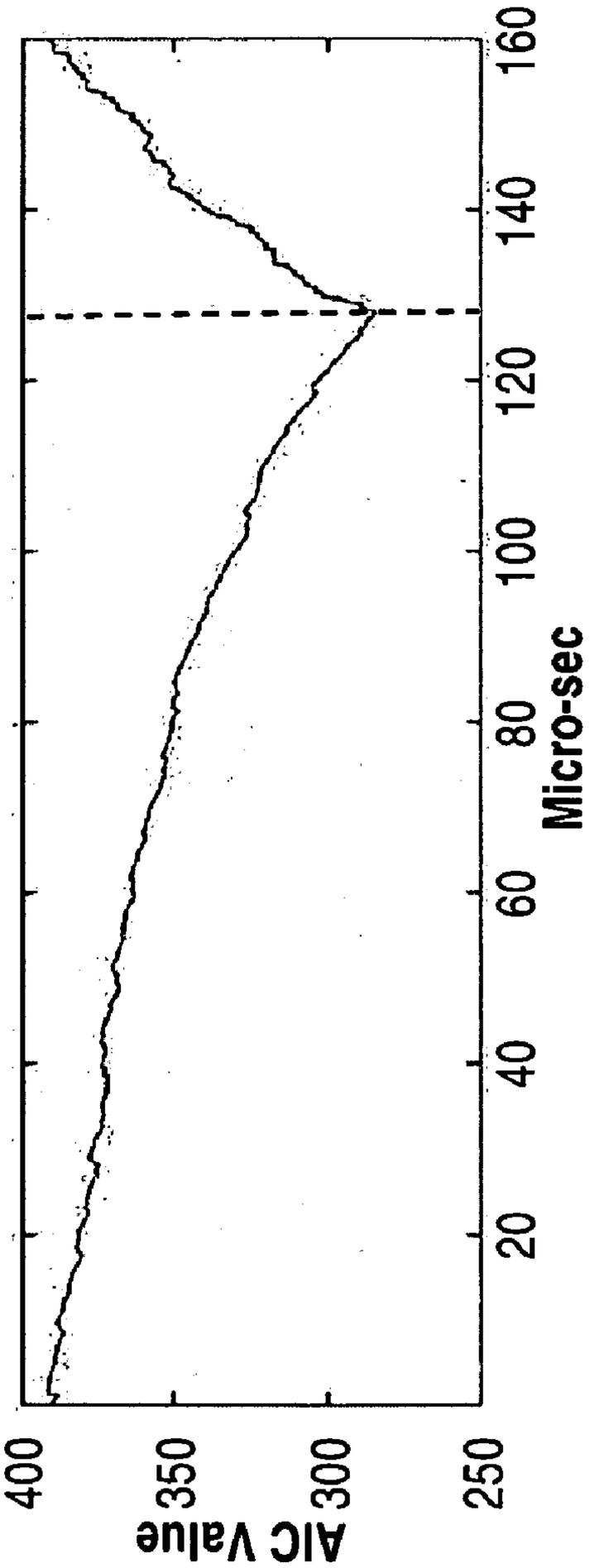

FIG. 12B

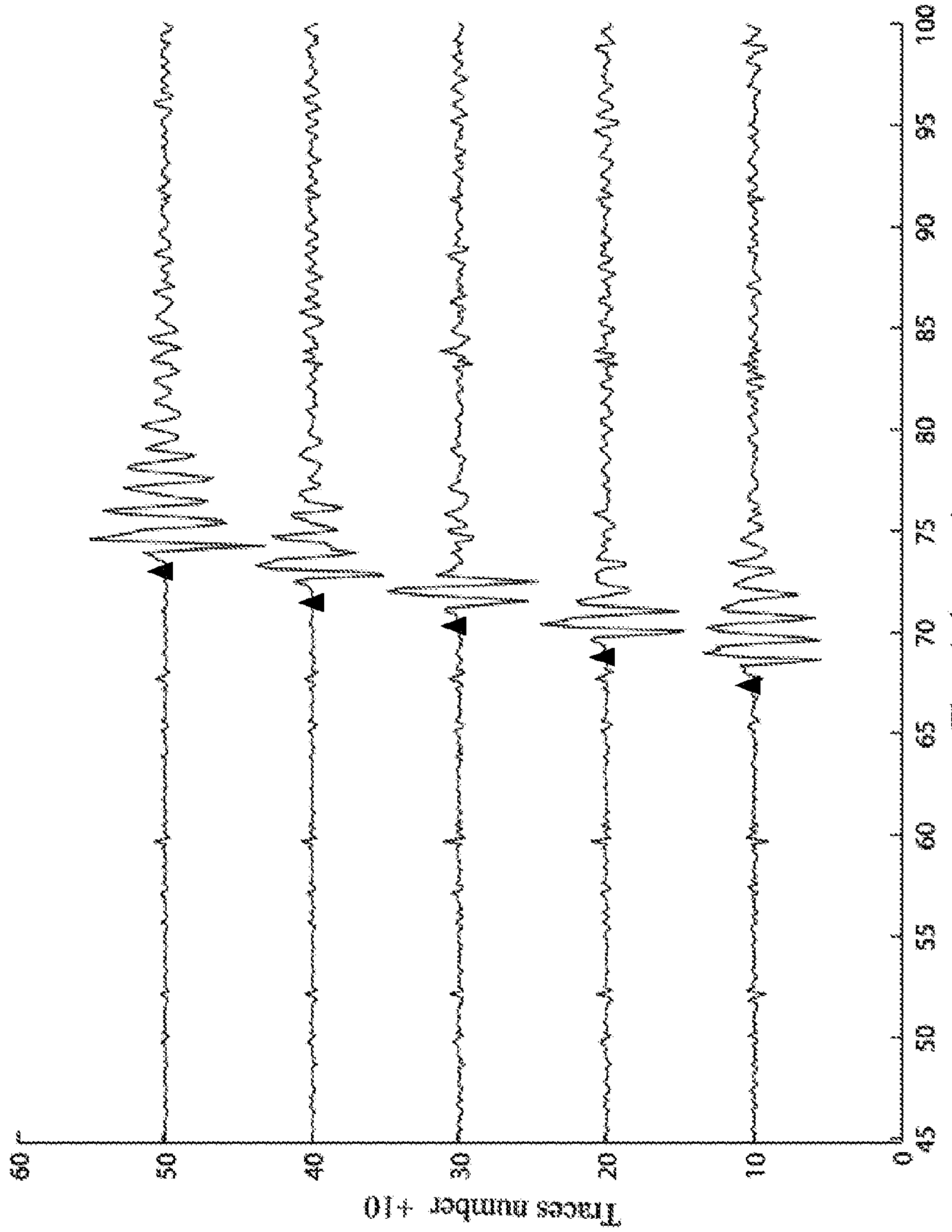
Traces number +10
60
50
40
30
20
10
0
45
50
55
60
65
70
75
80
85
90
95
100
Time (micro-sec)

FIG. 13

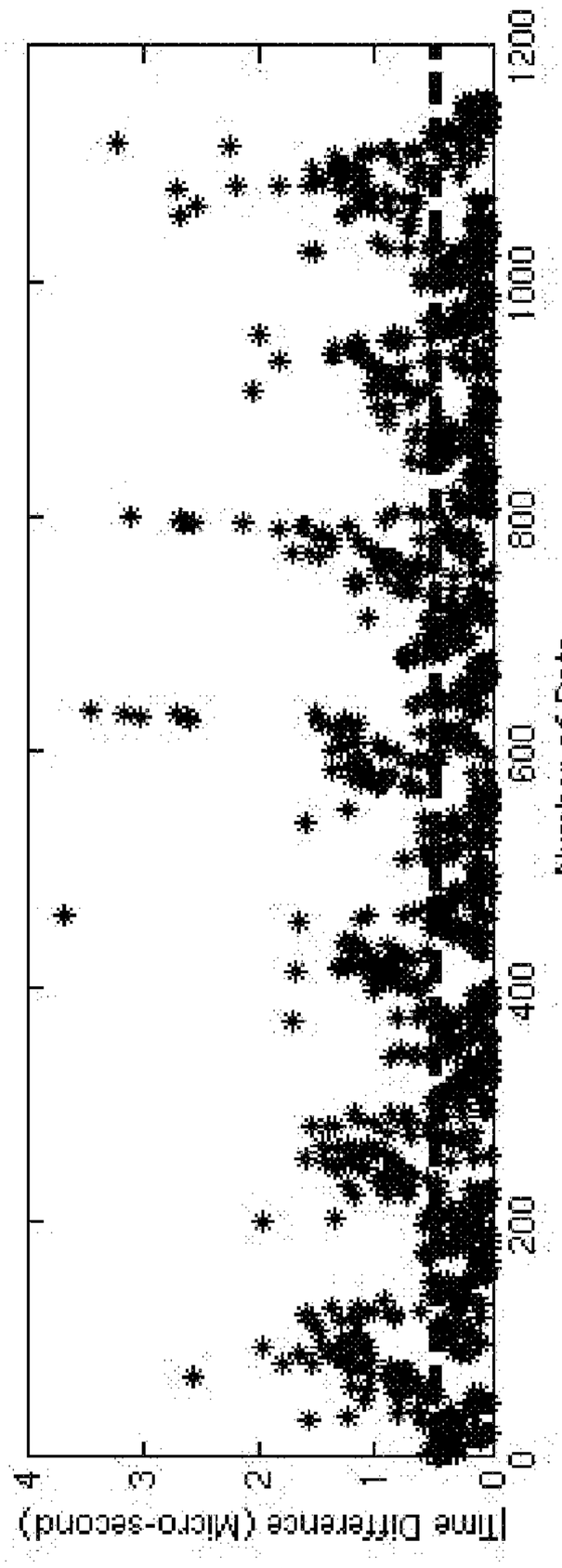

FIG. 14A

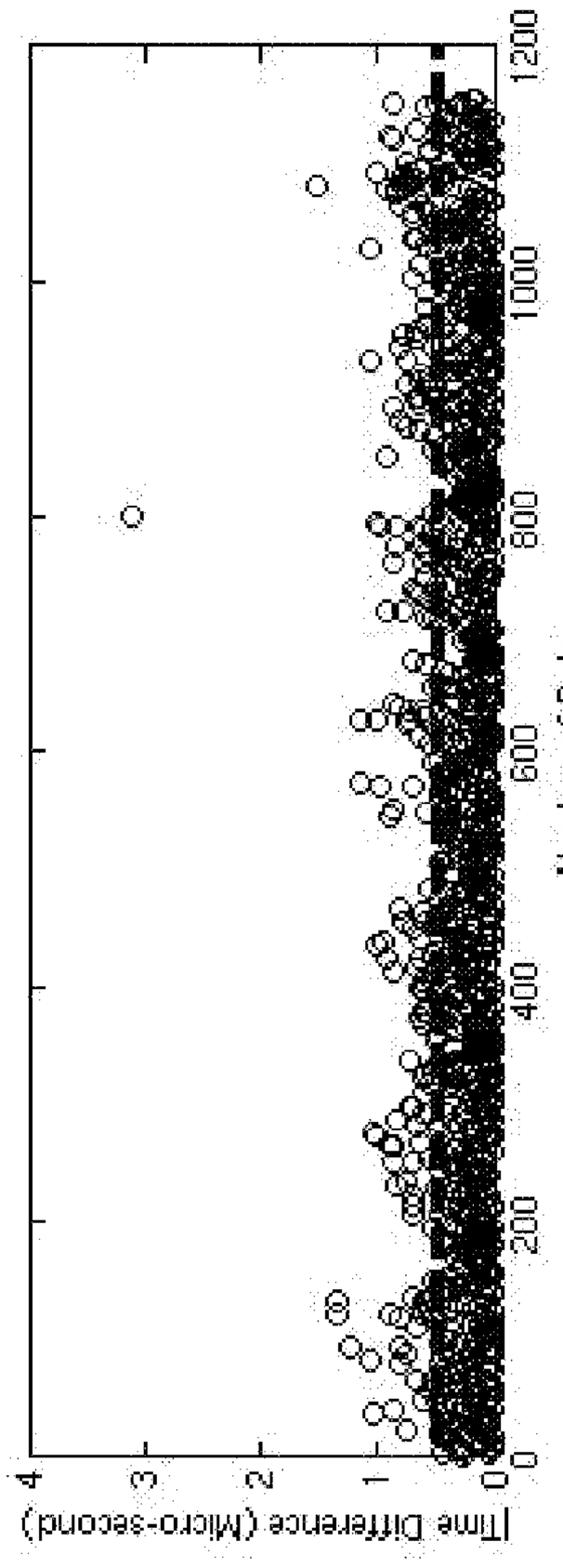

FIG. 14B

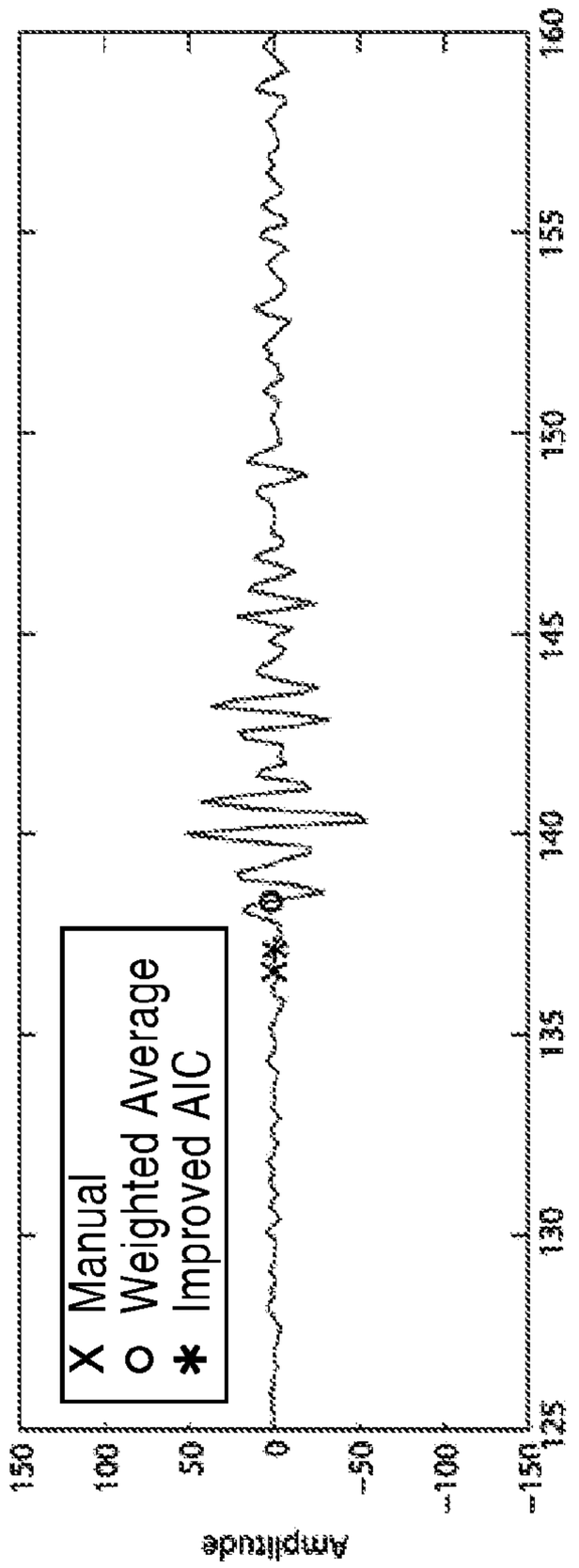

FIG. 15A

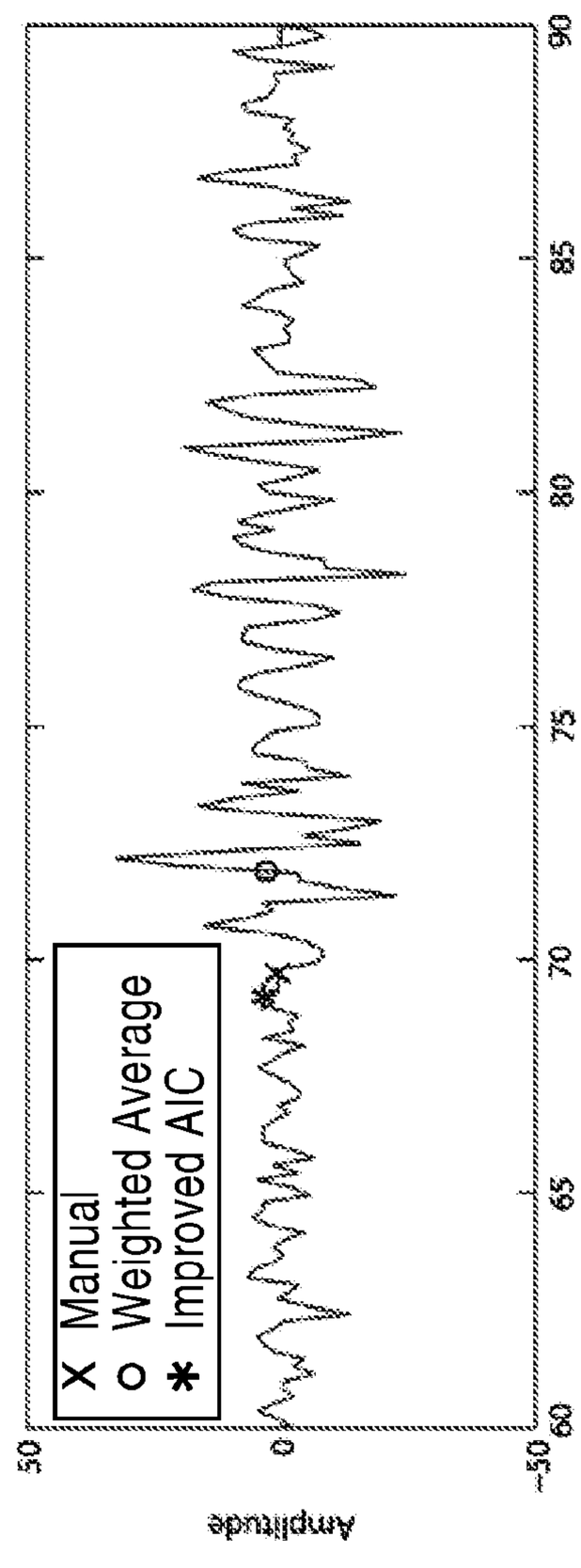

FIG. 15B

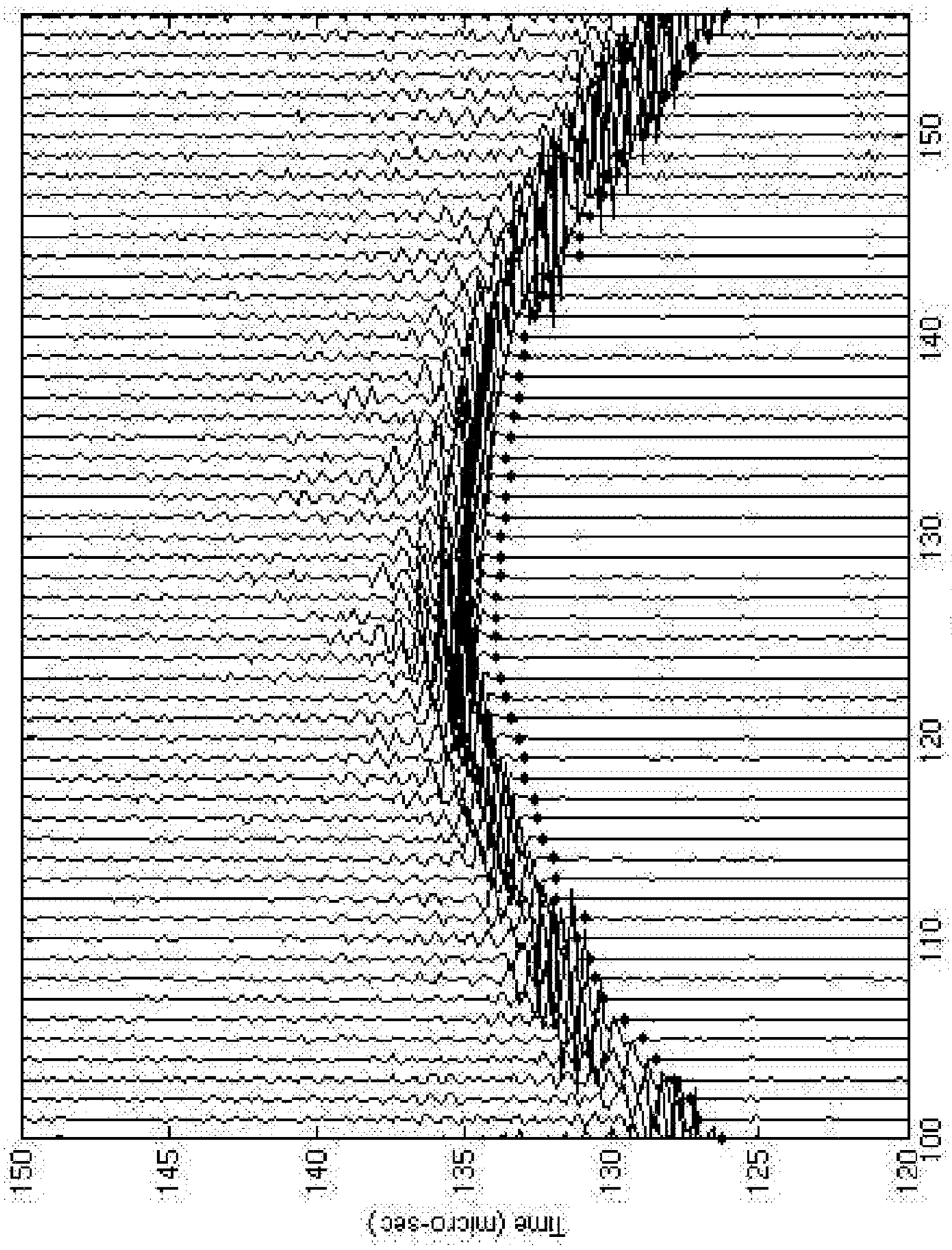
150
140
130
120
110
Receiver
150
145
140
135
130
125
120
100
Time (micro-sec)

FIG. 16

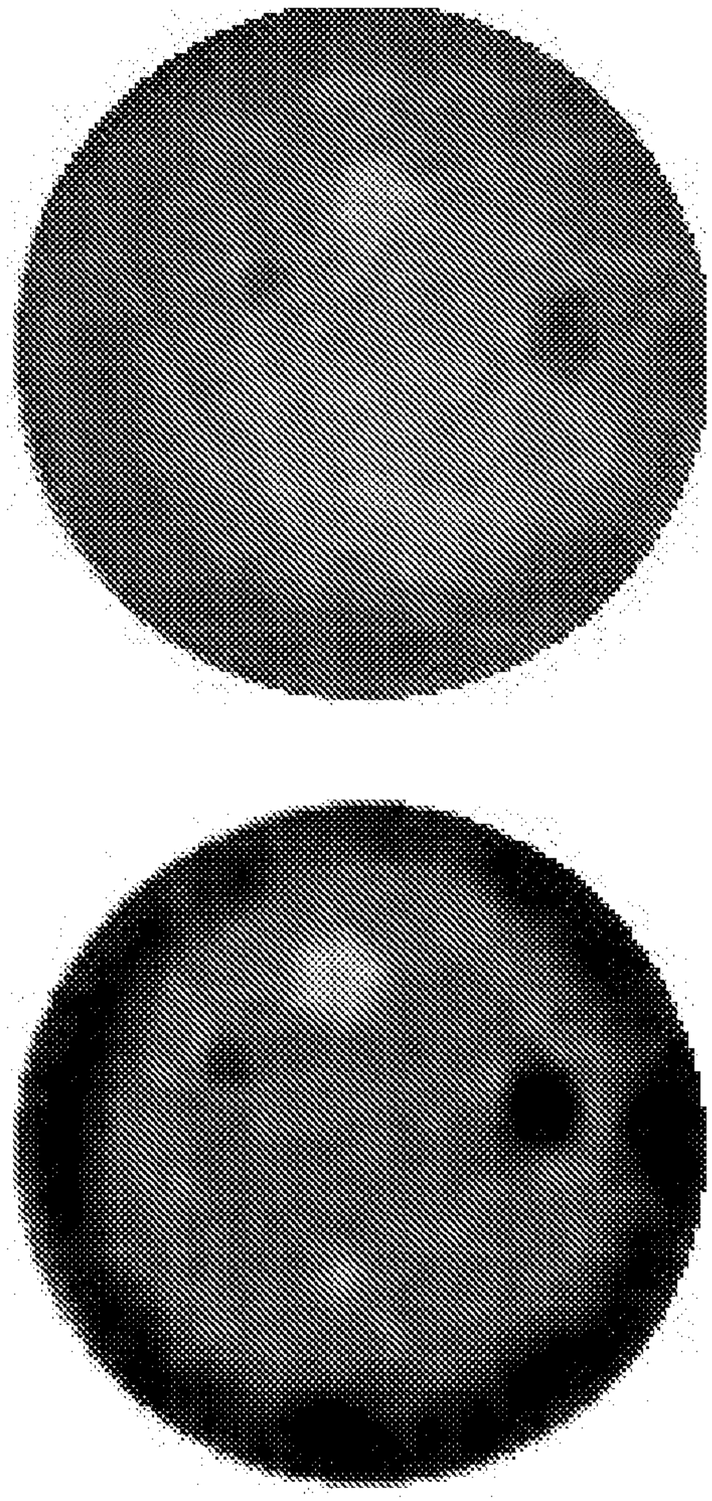

FIG. 17

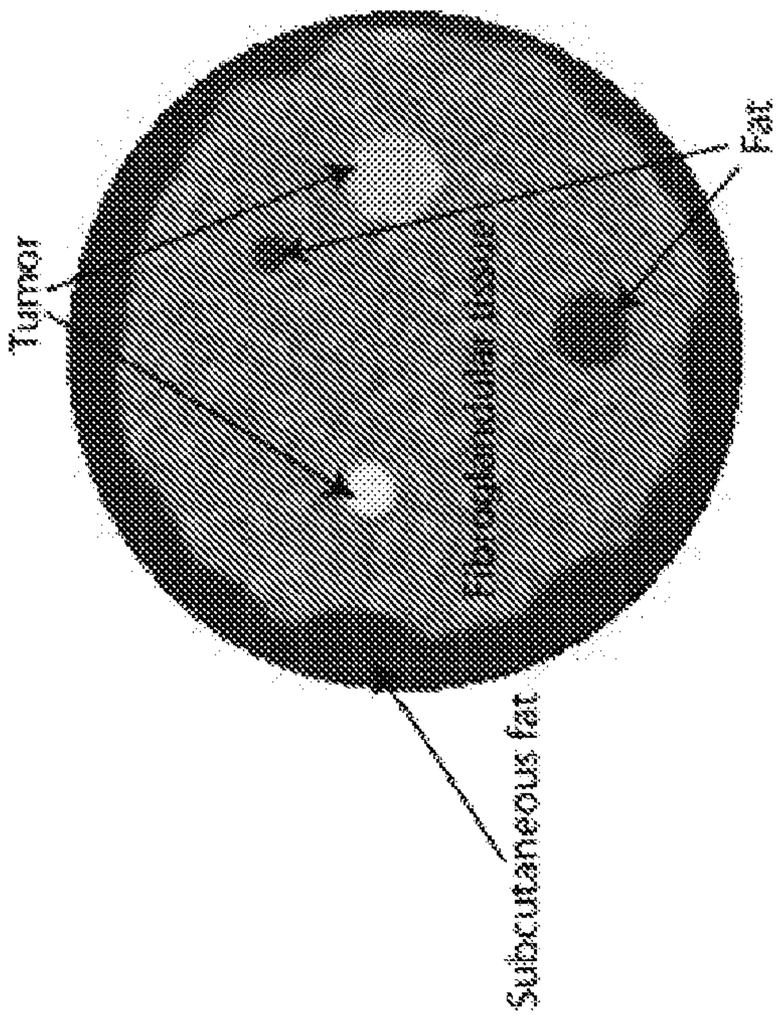

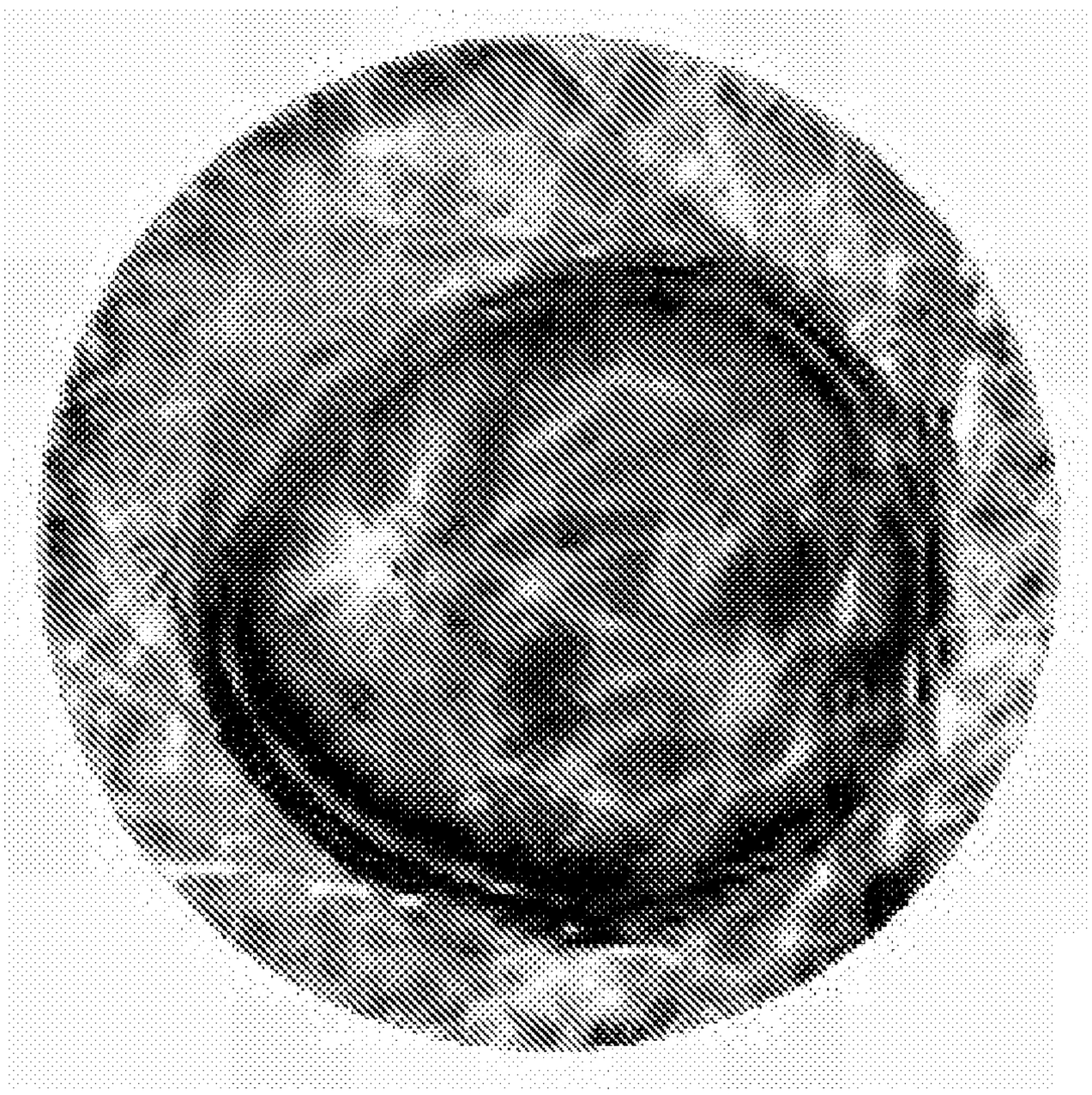

FIG. 18B

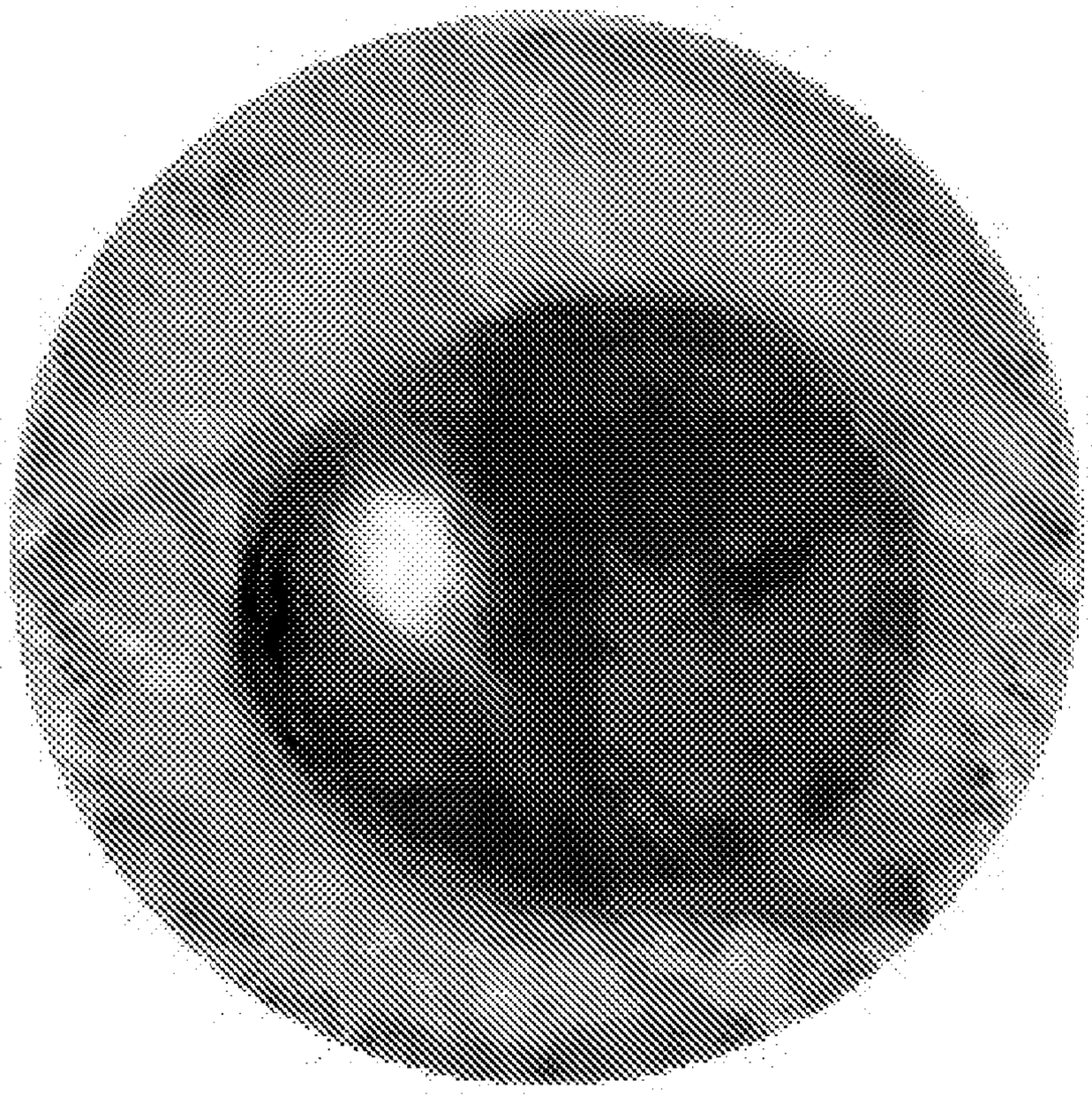

FIG. 18A

FIG. 19B

FIG. 19A

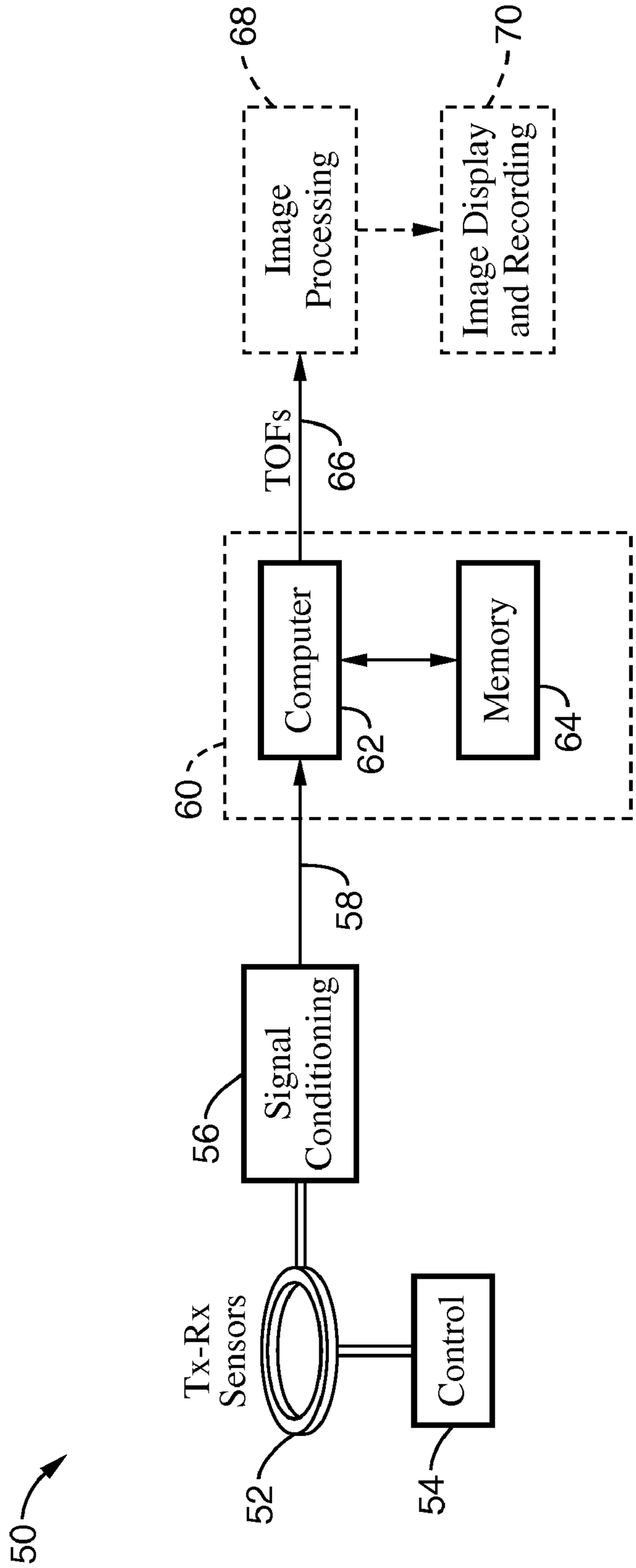
50
Tx-Rx Sensors
52
Signal Conditioning
56
58
Control
54
60
Computer
62
Memory
64
TOFs
66
Image Processing
68
Image Display and Recording
70

FIG. 20

AUTOMATIC TIME-OF-FLIGHT SELECTION FOR ULTRASOUND TOMOGRAPHY

CROSS-REFERENCE TO RELATED APPLICATIONS

[0001] This application claims priority from U.S. provisional patent application Ser. No. 60/901,903 filed on Feb. 16, 2007, incorporated herein by reference in its entirety.

STATEMENT REGARDING FEDERALLY SPONSORED RESEARCH OR DEVELOPMENT

[0002] This invention was made with Government support under Contract No.
[0003] DE-AC52-06NA25396, awarded by the Department of Energy. The Government has certain rights in this invention.

INCORPORATION-BY-REFERENCE OF MATERIAL SUBMITTED ON A COMPACT DISC

[0004] Not Applicable

NOTICE OF MATERIAL SUBJECT TO COPYRIGHT PROTECTION

BACKGROUND OF THE INVENTION

[0006] 1. Field of the Invention
[0007] This invention pertains generally to ultrasound imaging, and more particularly to automatic time-of-flight selection for ultrasonic signals.
[0008] 2. Description of Related Art
[0009] Ultrasonic imaging is used in a wide variety of medical and clinical applications. Image formation in ultrasonography is provided in response to analysis of the time-of-flight and the angle of incidence of the reflected ultrasound signals. It will be recognized that multi-path reflections often arise between the target object and the transducer, such as in response to highly reflective acoustic interfaces. These multi-path reflections interfere with proper image formation. For example, a prolongation of time-of-flight can lead to overestimation of the target object depth within the body. In addition, changes to the angle of incidence of the incoming sound signals cause aliasing in the calculated target object position. Therefore, in many cases the reflected sound waves are subject to both straight-line propagation as well as multi-path reflections at the same time. In order to overcome these problems ultrasonic imaging techniques have been developed in which a skilled operator can select which time-of-flight values result in generating the proper image.
[0010] Manual selection of time-of-flight (TOF) during ultrasonic imaging is presently considered the best method of achieving optimum image quality. However, this operator dependent process is very time-consuming when processing a large amount of ultrasound data, such as in the case of medical ultrasound tomography which may involve many thousand signals to be resolved. Inaccurate time-of-fight picks can result in noisy reconstructed sound-speed images with erroneous information about tumors, leading to wrong cancer detection and diagnosis.
[0011] Accordingly, a need exists for a system and method for operator independent time-of-flight selection for ultrasound imaging. These needs and others are met within the present invention, which overcomes the deficiencies of previously developed ultrasound imaging systems and methods.

BRIEF SUMMARY OF THE INVENTION

[0012] A method and system is described for operator-independent selection of time-of-flight (TOF) ultrasound signals, such as for a clinical imaging system using ultrasound sound-speed tomography. The invention provides a robust and computationally efficient solution which can be applied to replacing operator selected time-of-flights in various ultrasound systems. The automatic TOF "picker" is based on the Akaike Information Criterion (AIC). A preferred embodiment of the invention method utilizes an approach termed multi-model inference (model averaging), which is based on calculating AIC values across range of weighted models toward improving the accuracy of TOF picks. In one aspect a median filter is afterward utilized to eliminate outliers in the TOF picks. In another aspect of the invention, if the sensor system is symmetrical, such as a ring, then the reciprocal nature of signals is compared with TOFs being adjusted accordingly, such as averaging the reciprocal signals which exceed certain boundary conditions.
[0013] The method and apparatus provides an operator-independent, computationally efficient, and robust picker, which can accurately and reliably pick time-of-flights for clinical ultrasound signals, even for those with low signal-to-noise ratios.
[0014] The invention is amenable to being embodied in a number of ways, including but not limited to the following descriptions.
[0015] One embodiment of the invention can be generally described as a method of selecting time-of-flight (TOF) for ultrasound tomography waveforms generated by a given ultrasound tomography transmitter-receiver device directed on a tissue sample, comprising: (a) receiving a plurality of ultrasound waveforms from an ultrasound tomography transmitter-receiver device; (b) determining Akaike Information Criterion (AIC) values within a predetermined time window; and (c) selecting TOF for each the ultrasound waveform in response to the application of wavelet transforms searching the time window.
[0016] In one aspect of the invention, the AIC value can be determined in response to the best-model in which the AIC value is minimized. However, preferably, the AIC value is determined in response to multi-model averaging in which a weighted average of models is generated; and in which the weights for each model are assigned in response to the relative accuracy of each candidate model within the multiple models being considered.
[0017] The predetermined time window comprises a timing window which is preferably determined in response to transmitter-receiver geometry and the sound speed in water.
[0018] The set of TOF picks is preferably filtered to eliminate outliers in the TOF picks, for example by utilizing median filtering, which in one mode is configured to have a length customized to the time differences between picked TOFs and the corresponding calculated TOFs in water based on the ring array geometry. In one mode of the invention, the filtered out values are replaced with median values.

[0019] In one aspect of the invention, TOFs of reciprocal transmitter-receiver pairs are compared and the values of the associated TOF picks are adjusted if they exceed a given threshold. In one mode the threshold can be selected by a user based on individual requirements and data quality needs. In at least one implementation, adjusting of the TOF picks comprises replacing the TOF and its reciprocal TOF with an average of both TOF values.

[0020] In at least one implementation the AIC value is determined by comparing AIC values based on a series of models which have been previously specified.

[0021] Implementations of the present apparatus and/or method can be incorporated into various ultrasound systems, such as those generating ultrasound tomograph imaging in response to the TOF selections. By way of example, these systems may be configured for performing ultrasonic breast tomography. The inventive system and method is configured to provide operator-independent, automatic, determination of TOFs for a set of ultrasonic signals. In the method and system of the invention, TOFs are selected without necessitating manual picking of timing in each of the plurality of ultrasonic waveforms.

[0022] At least one implementation of the invention comprises a method of selecting time-of-flight (TOF) for ultrasound tomography waveforms generated by a given ultrasound tomography transmitter-receiver device directed on a tissue sample, comprising: (a) receiving a plurality of ultrasound waveforms from an ultrasound tomography transmitter-receiver device; (b) determining a predetermined time window using the sound speed of water for the given transmitter-receiver device; (c) determining Akaike Information Criterion (AIC) values for the received data within the predetermined time window; (d) calculating a weighted average model for the signal segment; (e) selecting a TOF for each the ultrasound waveform in response to the application of wavelet transforms searching the time window; (f) applying a median filter to the TOF selections; and (g) correcting each TOF associated with the plurality of ultrasound waveforms in response to the difference between reciprocals.

[0023] At least one implementation of the invention is an apparatus for processing ultrasound tomography waveforms, comprising: (a) means for receiving a plurality of ultrasound waveforms from an ultrasound tomography transmitter-receiver device directed through a tissue sample; (b) a computer processor and memory coupled to the receiving means; (c) programming executable on the processor for, (c)(i) determining a predetermined time window, (c)(ii) determining Akaike Information Criterion (AIC) values within the predetermined time window, and (c)(iii) selecting TOF for each the ultrasound waveform in response to the application of wavelet transforms searching the time window.

[0024] At least one implementation of the invention is a computer-readable media executable on a computer apparatus configured for processing ultrasound tomography waveforms, comprising: (a) a computer readable media containing programming executable on a computer processor configured for processing ultrasound tomography waveforms in response to receiving a plurality of ultrasound waveforms from at least one ultrasound tomography transmitter-receiver device directed through a tissue sample, in which the programming executable on the processor configured for, (a)(i) determining a predetermined time window, (a)(ii) determining Akaike Information Criterion (AIC) values within the predetermined time window, and (a)(iii) selecting TOF for each the ultrasound waveform in response to the application of wavelet transforms searching the time window.

[0025] The present invention provides a number of beneficial aspects which can be implemented either separately or in any desired combination without departing from the present teachings.

[0026] An aspect of the invention is an operator-independent method of selecting time-of-flight signals within an ultrasonic imaging device.

[0027] Another aspect of the invention is a time-of-flight selection method which utilizes multi-model inference in selecting time-of-flight.

[0028] Another aspect of the invention is a time-of-flight selection method which uses calculated AIC values within multi-modal inference.

[0029] Another aspect of the invention is a time-of-flight selection method which uses a median filter to eliminate outliers in the TOF picks.

[0030] Another aspect of the invention is a time-of-flight selection method which utilizes wavelet-AIC according to a weighted average model instead of the 'best model'.

[0031] Another aspect of the invention is a time-of-flight selection method which operates by removing outliers of the TOF picks using filtering, such as a median filter.

[0032] Another aspect of the invention is a time-of-flight selection method which performs no signal preprocessing which can introduce signal distortion effects due to filtering and wavelet de-noising.

[0033] A still further aspect of the invention is a method that can be implemented as hardware, software, or computer readable media, for processing waveforms in response to ultrasonic tissue imaging.

[0034] Further aspects of the invention will be brought out in the following portions of the specification, wherein the detailed description is for the purpose of fully disclosing preferred embodiments of the invention without placing limitations thereon.

BRIEF DESCRIPTION OF THE SEVERAL VIEWS OF THE DRAWING(S)

[0035] The invention will be more fully understood by reference to the following drawings which are for illustrative purposes only:

[0036] FIG. **1** is a flow diagram of time-of-flight selection according to an aspect of the present invention.

[0037] FIG. **2**A is a graph of absolute TOF differences between the manual picks and amplitude threshold picks.

[0038] FIG. **2**B is a graph of absolute TOF differences between the manual picks and AIC TOF picks according to an aspect of the present invention.

[0039] FIG. **3**A-**3**B are graphs of TOF picks within high and low signal-to-noise ratio images, showing a comparison of manual picks, amplitude threshold picks and AIC picks.

[0040] FIG. **4** is a graph of TOF picks according to an aspect of the present invention, showing arrival timing for a plurality of signals.

[0041] FIG. **5**A-**5**C are tomographic images acquired by X-ray CT (FIG. **5**A), and TOFs according to AIC method (FIG. **5**B) and the amplitude threshold method (FIG. **5**C).

[0042] FIG. **6**A-**6**B are tomographic images acquired using the sound-speed reconstruction method according to the present invention (FIG. **6**A) in comparison with sound-speed reconstruction using amplitude threshold picks (FIG. **6**B).

[0043] FIG. **7**A is a schematic image of a ring transducer array from which ultrasonic tomographic data was gathered.

[0044] FIG. **7**B is a schematic diagram of ultrasound pulse interaction within a ring transducer as shown in FIG. **7**A, showing scattering of the ultrasound field from transmitter to receiver.

[0045] FIG. **8** is a graph comparing picks based on best model ("O"), manual pick ("X"), and weighted average ("*"), showing a magnified section of the signal containing the TOF picks.

[0046] FIG. **9**A-**9**B are images of travel time differences between TOF picks according to an aspect of the present invention and the corresponding calculated TOFs in water based on the ring array geometry in FIG. **9**A and post processed version of that data in FIG. **9**B, showing data being median filtered and reciprocal pair checked.

[0047] FIG. **9**C-**9**D are images of sound-speed reconstructions for an ultrasound breast dataset corresponding to the TOF data in FIG. **9**A and FIG. **9**B respectively.

[0048] FIG. **10**A-**110**C are graphs of distortions arising from band-pass filtering and wavelet de-noising of raw ultrasound data (FIG. **10**A), second order zero-phase Butterworth band-pass filtered ultrasound data (FIG. **10**B), and wavelet de-noised ultrasound data (FIG. **10**C) according to aspects of the present invention.

[0049] FIG. **11**A-**11**B are graphs of amplitude and AIC value, respectively, prior to adding of random noise within a high SNR synthetic ultrasound waveform.

[0050] FIG. **12**A-**12**B are graphs of amplitude and AIC value, respectively, which are like those of FIG. **11**A-**11**B, to which random noise has been introduced.

[0051] FIG. **13** is a graph of five waveform snapshots of manual picking windows, showing solid triangles at the location of the manual TOF picks.

[0052] FIG. **14**A-**14**B are graphs of absolute TOF differences between manual picks and amplitude threshold picks (FIG. **14**A), and absolute TOF differences between manual picks and wavelet-AIC picks according to the present invention (FIG. **14**B).

[0053] FIG. **15**A-**15**B are graphs of TOF pick comparisons between manual picks, amplitude threshold picks and wavelet-AIC picks according to the present invention, showing use in a high SNR waveform (FIG. **15**A), and a low SNR waveform (FIG. **15**B).

[0054] FIG. **16** is a graph of an overlay of TOF picks according to an embodiment of the present invention, showing dots indicating the location of the TOF picks.

[0055] FIG. **17**A-**17**C are tomography images of a breast phantom compared with an X-ray CT scan (FIG. **17**A), ultrasound image with TOFs picked by the improved AIC picker according to the present invention (FIG. **17**B), and ultrasound image using amplitude threshold picks (FIG. **17**C).

[0056] FIG. **18**A-**18**B are tomography images of low SNR data using TOF picks according to the present invention (FIG. **18**A), and using amplitude threshold picks (FIG. **18**B).

[0057] FIG. **19**A-**19**B are tomography images of low SNR data using TOF picks according to the present invention (FIG. **19**A), and using amplitude threshold picks (FIG. **19**B).

[0058] FIG. **20** is a block diagram of an ultrasonic tomography device according to an aspect of the present invention, shown for processing a plurality of waveforms from which TOFs are automatically selected.

DETAILED DESCRIPTION OF THE INVENTION

[0059] Referring more specifically to the drawings, for illustrative purposes the present invention is embodied in the apparatus generally shown in FIG. **1**, **2**B, **3**A-**3**B, **4**, **5**B, **6**B, **8**-**12**B, **14**B, **15**A-**15**B, **16**, **17**B, **18**A, **19**A and **20**. It will be appreciated that the apparatus may vary as to configuration and as to details of the parts, and that the method may vary as to the specific steps and sequence, without departing from the basic concepts as disclosed herein.

Section A

[0060] 1. Introduction.

[0061] The wavelet-AIC (Akaike Information Criterion) picker is based on an autoregressive (AR) AIC picker that assumes an ultrasound signal can be divided into locally stationary segments and that the segments before and after the TOF represent two different stationary processes. Classically, the wavelet-AIC picker applies a running window and a wavelet transform to continuously search for an appropriate time window for the final TOF picking. Data points within the selected time window are divided into two segments at each data point i (i=1, . . . , k, . . . , N, where N is the total number of data points in the selected time window). To calculate the AIC function directly from the waveform for a given data point k the wavelet-AIC picker uses the formula of N. Maeda, found in the publication "A Method for Reading and Checking Phase Times in Autoprocessing System of Seismic Wave Data, Zisin", Journal of Seismological Society of Japan **38** (1985) 365-379, to yield the following:

$$\mathrm{AIC}(k)=k\log(\mathrm{var}(S(1,k)))+(N-k-1)\log(\mathrm{var}(S(k+1,N))) \quad (1)$$

where S(1,k) (for data points 1 through k) and S(k+1, N) (for data points k+1 through N) are the two segments in the selected time window, and the variance function "var(.)" is calculated using:

$$\mathrm{var}(S(i,j))=\sigma^2_{j-i}=\frac{1}{j-i}\sum_{l=i}^{j}(S(l,l)-\bar{S})^2, \quad (2)$$

$$i\le j,\ i=1,\ \ldots\ ,N \text{ and } j=1,\ \ldots\ ,N$$

where $\bar{S}$ is the mean value of S(i,j). The AIC value given by Eq. (1) measures the information loss of the selected model to approximate reality.

[0062] The point with minimum AIC value (e.g., minimum information loss, therefore referred to as 'best model') is selected to be the TOF point in the wavelet-AIC auto-picker of H. Zhang, C. Thurber and C. Rowe, in the article entitled "Automatic P-Wave Arrival Detection and Picking with Multiscale Wavelet Analysis for Single-Component Recordings" published in the Bulletin of the Seismological Society of America, vol. 93 (2003) pages 1904-1912.

[0063] The automatic wavelet-AIC TOF picker concept is then further improved according to the present invention by: (1) determining TOFs according to a weighted average model instead of the 'best model'; (2) removing outliers of the TOF picks using a median filter; and (3) eliminating effects of signal distortion due to filtering and wavelet de-noising which arises during data preprocessing, wherein signal-to-noise ratio (SNR) is improved.

[0064] 2. Using a Weighted Average Model to Determine TOFs.

[0065] FIG. **1** illustrates an embodiment **10** for an AIC picker method of the invention. A predefined window is calculated (determined) using the sound speed of water as represented by block **12**. In block **14** the AIC value is calculated (determined) for the original data within the predefined window. A weighted average is then computed as per block **16** for the signal segment in the time window. From the above information a time-of-flight is then determined at block **18**, and the

process is repeated at block **20** for all waveforms. In block **22** a median filter is preferably applied to the TOFs, for example with the filtered out (rejected) TOFs **24** being preferably replaced at block **26** with median values. Accepted TOFs **28** and replaced median values **26** are received in block **30** in which TOFs of reciprocal transmitter-receiver pairs are compared. If the difference values are less than or equal to a given threshold as per block **32**, then the TOFs are output at block **34**. Otherwise, when the differences are greater than the threshold as determined in block **36**, then the TOF values are discarded at block **38**. The following discusses in more detail aspects of the invention.

[0066] AIC value itself has no physical meaning and it becomes valuable only when compared across a series of models which are a priori specified. The model with the minimum AIC value is the best among all models being compared ("best model"). The measure associated with the AIC value that can be used to compare models is the normalized Akaike weights, as found in Eqs. (3) and (4), which indicate the relative importance of candidate models. In most cases, the best model (corresponding to the minimum AIC value) may have competitors for the top rank. An elegant solution to making an inference based on the entire set of models is to compute the weighted average based on the model uncertainties (i.e., Akaike weights), which is termed model averaging or model inference.

[0067] The running window for the prior uses of a wavelet-AIC picker are not necessary for use in clinical ultrasound data. An appropriate time window used for the TOF pick can be well defined based on the transmitter-receiver geometry and the sound-speed of water since sound-speed of tissue (e.g., breast tissue) is very close to that of water. The original geologic wavelet-AIC picker picks the point corresponding to the best model within the predetermined time window as the TOF. To incorporate all the information near the best model, weighted model averaging is applied to pick the TOF in the following sequence:

[0068] (1) Calculate AIC values (AIC_i, i=1, . . . n) for a series of data points near the point with the minimum AIC (AIC_{min}) using Eq. (1).

[0069] (2) Obtain the differences between AIC_i(i=1, . . . n) and AIC_{min}:

$$\Delta_i = AIC_i - AIC_{min} \tag{3}$$

[0070] (3) Compute the Akaike weights for each data point within the time window:

$$w_i = \frac{\exp(-\Delta_i/2)}{\sum_{r=1}^{n} \exp(-\Delta_r/2)} \tag{4}$$

[0071] (4) Obtain the TOF value using the weighted average:

$$t_{onset} = \sum_{i=1}^{n} w_i t_i \tag{5}$$

where t_i (i=1, . . . n) are the corresponding travel times for those points discussed in (1)-(3) and wi is obtained using Eq. (4).

[0072] When there is a sharp global minimum, the AIC value that indicates a high SNR, the difference between the average model pick and the best model pick is negligible. However, if the global minimum is not very sharp, which indicates a low SNR, the weighted average model can pick the TOF more accurately that the best model pick. This is the primary advantage of the automatic TOF picking method based on the weighted model averaging scheme.

[0073] 3. Removing Outliers of TOF Picks.

[0074] To remove outliers in the TOF picks, the TOF picks are first compared for the reciprocal transmitter-receiver pair. The reciprocal transmitter-receiver pair means that two transducers in the ring array transmit and receive signals in opposite directions; which is typically possible in that most sensor heads are symmetrical, such as radially symmetrical. Ideally, the TOF picks for a reciprocal pair should be the same, however, this rarely occurs in practice. In the data cleaning process according to the present invention, if the TOF difference for the reciprocal pair exceeds a predefined threshold, then the TOF picks are adjusted, for example replacing both TOF picks by the average of the two TOF picks. The predefined threshold value can be customized by users based on their individual requirements and data quality needs.

[0075] To eliminate outliers in the TOF picks more effectively, this embodiment applies a median filter with a customized length to the time differences (TD) between the TOFs picked according to the invention and the corresponding calculated TOFs in water based on the ring array geometry.

[0076] Although other techniques can be utilized without departing from the teachings of the present invention, the median filter is a particularly well-suited tool for reducing "salt and pepped" noise (outliers). To take advantage of this property and the continuity property of a TOF surface (formed by TOFs of all transmission data), TDs are rearranged into a 2-D matrix in such a way that each row represents the TD values for a single transmitter, and TD values for adjacent transmitters in the ring array are put into adjacent rows (except the first and last transmitter due to the circular geometry of the ring). This rearrangement results in a 256 by 256 matrix (D). Another 256 by 256 matrix (M) containing all median values is calculated with a sliding window of the same size as the median filter. Adaptive thresholds for the median filter are set up by calculating the standard deviation (STD) and the mean value (ME) of TDs:

$$\text{TolMin} = \text{ME} - f^{*}\text{STD},$$
$$\text{TolMax} = \text{ME} + f^{*}\text{STD}. \tag{6}$$

where To/Min and To/Max are the minimum and maximum tolerance of time differences, respectively, and f is a customized scale factor of the standard deviations with a value between 0 and 1. The median filter based on the above thresholds is applied to the matrix D: if D(i,j)−M(i,j)<TolMin or D(i,j)−M(i,j)>TolMax, the corresponding picked TOF is replaced with the median value; otherwise, it is discarded.

[0077] 4. Eliminating Distortion of Filtering and Wavelet De-noisin.

[0078] Filtering and techniques for elimination of noise (de-noising techniques) can be utilized to preprocess a signal to improve its signal-to-noise ratios (SNR). Original wavelet-AIC pickers were characterized by applying the wavelet de-noising to raw seismogram data before picking the TOF.

[0079] However, both the filtering and wavelet de-noising may distort a signal while attempting to increase the SNR. Due to the short transient time of ultrasound signals, a small distortion of the ultrasound waveform may result in large unwanted artifacts or erroneous information during TOF picking. For these reasons and in order to preserve the true shapes of ultrasound signal onsets as much as possible, a preferred embodiment of the present approach does not per-

form any data preprocessing toward improving signal-to-noise ratios (SNRs), because the improved automatic TOF picker described herein is configured to handle ultrasound data with low SNRs as demonstrated in the following.

[0080] 5. Capability to Handle Noisy Data.

[0081] To estimate the maximum amount of random noise that our improved wavelet-AIC TOF picker can tolerate, progressively increasing amounts of random noise were added to a synthetic ultrasound waveform with a similar spectrum to that of in vivo ultrasound breast data acquired by a ring transducer array. The average amplitudes of the random noise were, respectively, 0%, 20%, 40%, 60% and 80% of the maximum absolute amplitude of the synthetic ultrasound signal. The TOF picker according to the present embodiment was able to consistently detect the correct TOF in the presence of even 80% white noise, which corresponds to a 4.5 dB SNR. This is not surprising as the testing performed herein, as well as prior work on the AIC approach itself, indicate that AIC TOF pickers should be highly tolerant of relatively high noise levels if an appropriate time window is utilized.

[0082] 6. Experimental Results.

[0083] To assess the performance of the inventive improved AIC picker, TOFs picks according to the invention were compared with those of the traditional amplitude threshold picker, and manual picks on 1160 waveforms of in vivo ultrasound breast data acquired using a ring transducer array. Manual picking was conducted by an experienced expert who determined the TOF of each waveform by recognizing the first rise time of the signal, and thus serves as a standard of comparison.

[0084] FIG. **2**A-**2**B illustrate comparisons of TOF picking. FIG. **2**A illustrates the absolute time difference between manual picks and amplitude threshold picks. FIG. **2**B illustrates absolute time difference between manual picks and wavelet-AIC TOF picks according to the present invention. The statistics illustrate that for these 1160 in vivo ultrasound breast waveforms, over 85% of the TOFs picked by the improved wavelet-AIC picker of the present invention are within the three sample points from the manual picks. Among picks by the amplitude threshold picker, only 48% of them are within the three sample points from the manual picks. The dashed lines indicate the three sample point interval from manual picks.

[0085] Further analysis with more ultrasound data from breast examinations reveal that the performances of the improved wavelet-AIC picker of the current invention and amplitude threshold picker are more comparable for less noisy data, while in response to high noise level (or low SNRs) data, the accuracy of the amplitude threshold picker drops abruptly.

[0086] FIG. **3**A-**3**B illustrates two waveforms of different SNRs along with TOF picks utilizing picking by manual methods, amplitude threshold, and AIC techniques according to the present invention. The manual picks are designated by an "X", the weighted average picks with an "O", and the AIC picks marked by a "*". It will be noted that the AIC picks remain close to that of the manually selected standard of comparison. It can also be clearly seen that for the high SNR waveform of FIG. **3**A, the three TOF picks are reasonably close to one another, although the improved AIC pick of the invention are closer to the manual pick. FIG. **3**B illustrates a low SNR waveform showing a noisier waveform in which the amplitude threshold picker selected the wrong TOF, while the AIC picker of the invention remained comparable to that selected by the manual pick.

[0087] FIG. **4** illustrates an example of TOF pick overlays by the AIC picker of the present invention on corresponding in vivo ultrasonic breast waveforms. It should be noted that the solid dot on each waveform segment indicates the TOF pick for that waveform.

[0088] Tomograms obtained using improved wavelet-AIC picks according to the present invention are compared with those selected using amplitude threshold picks for in vitro and in vivo ultrasound datasets.

[0089] FIG. **5**A-**5**C illustrates a comparison between breast phantom images.

[0090] The X and Y axes in these example images span 220 mm in length. In FIG. **5**A a representative X-ray CT scan of a breast phantom is shown. In FIG. **5**B is a tomogram obtained using the improved AIC picks according to the invention. FIG. **5**C illustrates a tomogram obtained using amplitude threshold picks. It should be readily recognized that the tomogram of FIG. **5**B contains far fewer artifacts than in FIG. **5**C.

[0091] FIG. **6**A and FIG. **6**B illustrates a comparison of sound-speed tomograms for in vivo ultrasound breast data in which TOF picks are generated using TOF pick methods according to the present invention in FIG. **6**A and by utilizing amplitude threshold picks in FIG. **6**B.

Section B

[0092] Section A provided a description and summarization of aspects of the invention, while this section (Section B) describes aspects of the invention in large part from the original description. It should be appreciated that many of the equations and figures used herein may duplicate those found in Section A. Figure numbering is continued from Section A, but equation numbering is restarted for section B to provide consistency with the original text. Reference citation numbers are retained in this section to provide additional information.

[0093] 7. Section B: Introduction.

[0094] Ultrasound sound-speed tomography has great potential to detect and diagnose breast cancer. [1,2,3,4]. A clinical prototype of ultrasound breast-imaging system with a ring array, termed the Computed Ultrasound Risk Evaluation (CURE), has been developed at the Karmanos Cancer Institute, Wayne State University in Detroit, Mich. for ultrasound tomography [5].

[0095] FIG. **7**A is a schematic illustration of a ring transducer array performing ultrasonic imaging. In FIG. **7**B a schematic of Interaction of an ultrasound pulse with a target leads to a scattered ultrasound field from transmitter (Tx) to receiver (Rx).

[0096] In general, breast cancer has a higher sound-speed than the surrounding breast tissue. A primary purpose of CURE is to efficiently and reliably produce sound-speed images of the breast for cancer detection and diagnosis. A potential sound-speed reconstruction method for such a purpose is time-of-flight (TOF) ultrasound transmission tomography. Accurate picking of TOFs of ultrasound transmitted signals is an extremely important step to ensure high-resolution and high-quality reconstruction of the sound-speed distribution.

[0097] For each two-dimensional (2D) slice of ultrasound breast data, each element of the CURE device acts as a transmitter as well as a receiver, and all elements receive the scattered sound waves when one element transmits.

[0098] CURE acquires 70-80 slices of ultrasound data for whole breast imaging, resulting in a large volume of ultrasound data for each patient. Therefore, it is not feasible to manually pick TOFs of transmitted ultrasound data for sound-speed tomography because manual picking is too time-consuming (~600,000 waveforms needs to be analyzed for each patient). Accordingly, an automatic TOF picker which can properly identify TOF provides an important tool for ultrasound tomography, particularly for clinical applications.

[0099] Different automatic TOF pickers have been developed, in particular for use with geophysical applications to reconstruct the internal structure of the Earth. The techniques used in these devices fall into three general categories. The simplest method is the amplitude threshold picker that applies an absolute value of the threshold to the band-pass filtered signal. It is not applicable for data having low signal-to-noise ratios (SNRs). A variation is called "Short-Term-Average/Long-Term-Average (STA/LTA)" method using the signal's envelope [6]. The second type of auto-pickers utilizes a running window. Certain characteristics are repeatedly calculated within successive sections of the time series, producing a time dependent function. The TOF is usually identified by an obvious change in the behavior of this function ([7,8]). The third type of auto-picker relies on using the coherence characteristic between traces. One among these pickers convolves a shifting reference waveform with the signal. The TOF of the signal is determined when the measure of the quality of the match is a maximum. This method assumes that the signal is reasonably similar to the reference waveform. Several papers describe this type of picker, including [9,10,11].

[0100] In 1951 Kullback and Leibler [12] proposed what is now known as the Kullback-Leibler information criterion to measure the information loss when approximating reality using recorded data. In the 1970s, Akaike (cited in [13]) proposed a model selection criterion, the Akaike Information Criterion (AIC), which relates the maximum likelihood with the Kullback-Leibler information criterion and minimizes the information loss during model selection. Sleeman and Eck [14] applied the AIC and autoregressive (AR) techniques to detect the TOFs of seismograms, and their TOF picker is called AR-AIC picker. Autoregressive techniques are based on the assumption that a waveform can be divided into locally stationary segments as an AR process and the segments before and after the TOF point are two different stationary processes. On the basis of this assumption, the AR-AIC picker can be used to detect the TOF of a seismogram by analyzing the variation in AR coefficients. The AIC is usually used to determine the order of the AR process when fitting a time series. When the order of the AR process is fixed, the AIC is a measure of the model fit. In the AR-AIC picker, the order of the AR coefficient is determined on a trial and error basis (for details see [14]). To overcome this difficulty and inefficiency, Zhang et al. [8] proposed a wavelet-AIC picker in which the AIC values are calculated directly from the seismogram using Maeda's formula [15]. In this method, a running window and a wavelet transform are used to guide the AIC picker by finding the appropriate time window that includes the TOF point of a seismogram.

[0101] All the above techniques were historically developed to pick elastic signals, particularly seismic waves. However, these underlying concepts of these geologic mechanisms have not been utilized for automatically picking TOFs for in vivo medical ultrasound data. Kurz et al. [16] is one of the few who applied an auto-picker to acoustic emission in concrete.

[0102] An improved AIC automatic TOF picker is taught according to the present invention which is particularly well suited for in vivo ultrasound breast data based on the wavelet-AIC TOF picker described in [8]. The improved method makes use of an approach termed multi-model inference (model averaging), based on the calculated AIC values, to enhance the accuracy of TOF picks. Aspects of the present invention also investigate applying a median filter to remove TOF outliers. Demonstration of the inventive automatic TOF picker shows that it can accurately pick TOFs in the presence of random noise of up to 80% of the maximum absolute synthetic signal amplitude. The improved automatic TOF picking method is applied to clinical ultrasound breast data which demonstrates that ultrasound sound-speed tomography with our improved automatic TOF picks significantly enhances the reconstruction accuracy while reducing image artifacts.

[0103] 8. Ultrasound Breast Data Acquired Using the CURE Device.

[0104] The clinical ultrasound breast data used for this study was collected with the CURE device, a clinical prototype ultrasound scanner designed for clinical ultrasound breast tomography. CURE is capable of recording all ultrasound wavefields including reflected, transmitted, and diffracted ultrasonic signals from the breast tissue. The engineering prototype of CURE is described in [17], and the current clinical prototype is described in [5]. FIG. **7**A-**7**B are schematic representations of the transducer ring and Tx to Rx pattern for a given pulse. FIG. **7**B illustrates scattering of ultrasound emitted from a transducer element and received by all transducer elements along the ring. By way of example and not limitation, there are a total of 256 elements in this 20-cm diameter ring array. Each element is configured to emit and receive ultrasound waves with a central frequency of 1.5 MHz. During the scan, the ring array is immersed in a water tank, and encircles the breast. The signals are recorded at a sampling rate of 6.25 MHz. The whole breast is scanned slice by slice, and the scanned slice data are recorded by a computer for data processing afterwards. A motorized gantry is used to translate the ring along the vertical direction, starting from the chest wall to the nipple.

[0105] 9. Improved Automatic AIC Time-Of-Flight Picker.

[0106] The wavelet-AIC TOF picker [8] is based on the AR-AIC picker which assumes that a signal can be divided into locally stationary segments and that the segments before and after the time-of-flight point are two different stationary processes [14]. Data points within the selected time window are divided into two segments at each data point i(i=1, . . . , k, . . . N),where N is the total number of data points in the selected time window. For a given data point k the wavelet-AIC TOF picker uses Maeda's formula [15] to calculate the AIC function directly from the waveform:

$$\mathrm{AIC}(k)=k\log(\mathrm{var}(S(1,k)))+(N-k-1)\log(\mathrm{var}(S(k+1,N))) \quad (1)$$

where S(1,k) (for data points 1 through k) and S(k+1, N) (for data points k+1 through N) are the two segments in the selected time window, and the variance function "var(.)" is calculated using

$$\mathrm{var}(S(i,j))=\sigma^2_{j-i}=\frac{1}{j-i}\sum_{l=i}^{j}(S(l,l)-\bar{S})^2, \quad (2)$$

$$i\le j,\ i=1,\ldots,N \text{ and } j=1,\ldots,N$$

where S is the mean value of S(i,j).

[0107] The AIC value given by equation (1) measures the information loss of using the current selected model to approximate reality. In the wavelet-AIC auto-picker in [8], selecting the point with minimum AIC value indicates the minimum information loss, wherein it is called the best model, to be the TOF point.

[0108] The present invention provides improvements to automatic wavelet-AIC TOF picking according to each of the following, to be considered separately or in combination: (1) using a weighted average model instead of the best model to determine TOFs; (2) removing outliers of TOF picks using a median filter; and (3) eliminating effects of signal distortion due to filtering and wavelet de-noising during data preprocessing for improving SNR. A schematic flowchart of the improved AIC TOF picker according to the present invention has already been shown in FIG. **1** described in Section A. The details of the improved AIC method of the current invention are described in the following.

[0109] 9.1. Using a weighted average model to determine TOFs.

[0110] An AIC value by itself has no physical meaning and it becomes interesting only when it is compared to a series of a priori specified models [18]. The model with the minimum AIC value is the best among all models being compared. The measure associated with the AIC value that can be used to compare models is the normalized Akaike weights (Eqs. 3 and 4). Akaike weights indicate the relative importance of the candidate models. In most cases, the best model (corresponding to the minimum AIC value) may have competitors for the top rank. An elegant solution to make an inference based on the entire set of models is to compute the weighted average based on the model uncertainties (i.e. Akaike weights). This is referred to model averaging or model inference.

[0111] The running window used in for the wavelet-AIC TOF picker [8] is not necessary for clinical ultrasound data. An appropriate time window used for the TOF picks can be well-defined based on the transmitter-receiver geometry and the sound-speed of water since the sound-speed of breast tissue is close to that of water. To incorporate all the information near the best model, a weighted average model is utilized to pick the TOF in the following sequence:

[0112] (1) Calculate AIC values (AIC_i, i=1, . . . n) for a series of data points near the point with the minimum AIC (AIC_{min}) using equation (1).

[0113] (2) Obtain the differences between AIC_i(i=1, . . . n) and AIC_{min}:

$$\Delta_i = AIC_i - AIC_{min} \tag{3}$$

[0114] (3) Compute the Akaike weights for each data point within the time window:

$$w_i = \frac{\exp(-\Delta_i/2)}{\sum_{r=1}^{n} \exp(-\Delta_r/2)} \tag{4}$$

[0115] (4) Obtain the TOF value using the weighted average:

$$t_{TOF} = \sum_{i=1}^{n} w_i t_i \tag{5}$$

where t_i (i=1, . . . n) are the corresponding travel times for those points discussed in (1)-(3) and ω_i is obtained using equation (4).

[0116] When there is a sharp global minimum, the AIC value that indicates a high SNR, the difference between the TOF pick based on the weighted average model and that based on the best model is negligible. However, if the global minimum is not very sharp, which indicates a low SNR, the weighted average model can pick the TOF more accurately than picking based on the best model. This is one of the only advantages of the automatic TOF picking method based on the weighted model averaging scheme.

[0117] FIG. **8** illustrates an example of comparison among the TOF pick based on the best model, the TOF pick based on the weighted average model, and the manual pick of an in vivo ultrasound breast signal acquired using the CURE device. The circle ("○") represents the TOF picked with the best model, the cross ("X") corresponds to the manual pick of the TOF, and the asterisk ("*") is the TOF pick using the weighted average model. It can be seen that the latter is closer to the manual TOF pick than the pick based on the best model.

[0118] 9.2. Removing outliers of TOF picks.

[0119] To eliminate outliers of the TOF picks, a median filter is applied to the time differences (TDs) between the TOFs picked according to the present invention from ultrasound breast data and calculated using the water sound-speed and the ring array geometry. The median filter is a good tool for reducing 'salt and pepper' noise (outliers). To take advantage of this property and the continuity property of a TOF surface (formed by TOFs of all transmission data) ([19]), TDs are rearranged into a 2-D matrix such that each row represents the TD values for a single transmitter, and TD values for adjacent transmitters in the ring array are put into adjacent rows (except the first and last transmitter due to the circular geometry of the ring). This rearrangement results in a 256 by 256 matrix(D). Another 256 by 256 matrix (M) containing all median values of TOFs is calculated with a sliding window of the same size as the median filter. Adaptive thresholds for the median filter are set up by calculating the standard deviation (STD) and the mean value (ME) of TDs:

$$\text{TolMin} = \text{ME} - f^*\text{STD},$$
$$\text{TolMax} = \text{ME} + f^*\text{STD}. \tag{6}$$

where TolMin and TolMax are the minimum (could be a negative value) and maximum tolerance for TDs, respectively, and f is a given scale factor of the standard deviations with a value between 0 and 1. The median filter based on the above thresholds is applied to the matrix D: if D(i,j)-M(i,j) <TolMin or D(i,j)-M(i,j)>TolMax, then the corresponding picked TOF is replaced with the median value.

[0120] To further clean up the remaining picks, the TOF picks for the reciprocal transmitter-receiver pair are compared against each other. Reciprocal transmitter-receiver pair, here, means that two transducers in the ring array transmit and receiver signals in the opposite directions. Ideally, the TOF picks for the reciprocal pair should be the same, which rarely happens in practice. In the example data cleaning process, if the TOF's difference between the reciprocal pair exceeds a predefined threshold, both picks are discarded. The predefined threshold value can be customized by users based on their individual requirement and data quality.

[0121] FIG. **9**A-**9**B illustrates original matrix D and its post-processed version for an in vivo ultrasound breast data acquired using the CURE device. By way of this example

both x and y axes span 200 mm in length. Compared with FIG. **9**A, FIG. **9**B shows that the inconsistent picks and outliers are effectively eliminated.

[0122] FIGS. **9**C-**9**D are ultrasound sound-speed transmission tomography results for an in vivo ultrasound breast dataset using the TOF picks shown in FIGS. **9**A and **9**B, respectively. These figures demonstrates that the example TOF data cleaning procedure described above can effectively remove TOF outliers and greatly improve the quality of ultrasound TOF sound-speed tomography images.

[0123] 9.3. Signal distortion due to filtering and wavelet de-noising.

[0124] Filtering and de-noising techniques are usually used to preprocess a signal to improve its SNRs. The wavelet-AIC TOF picker [8] applies the wavelet de-noising to a raw seismogram before it picks the TOF. In fact, both the filtering and wavelet de-noising may distort a signal while attempting to increase the SNR [20].

[0125] FIG. **10**A-**10**C illustrates a comparison of a raw ultrasound data segment (FIG. **10**A) acquired with the CURE device with its filtered version (FIG. **10**B) and wavelet de-noised version (FIG. **10**C). The signal in FIG. **10**B was filtered using a second-order zero-phase Butterworth band-pass filter with the stop band corner frequencies at 0.3 MHz and 2.3 MHz, and the pass band corner frequencies at 0.9 MHz and 1.7 MHz. For the wavelet de-noised signal in FIG. **10**C, thresholding was applied to the wavelet coefficients using the Birge-Massart penalization method [21]. The solid vertical line in each of the figures represents the picked TOFs from the raw ultrasound data, while the dashed line indicates the picked TOFs from the filtered and de-noised segments.

[0126] Coincidently, TOFs picked from the band-pass filtered signal and the wavelet de-noised signal are the same as seen in Table 1. From FIG. **10**A-**10**C signal distortions due to the wavelet de-noising and zero-phase band-pass filtering can be seen. Because of the short transient time of ultrasound signals, a small distortion of the ultrasound waveform may result in large unwanted artifacts or erroneous information during TOF picking. For these reasons and in order to preserve the true shapes of ultrasound signal onsets as much as possible, no signal preprocessing is performed toward improving the SNRs, because the improved automatic TOF picker of the invention can handle ultrasound data with low SNRs as demonstrated in the following.

[0127] 9.4. Capability to handle noisy data.

[0128] To estimate the maximum amount of random noise that our improved wavelet-AIC TOF picker can tolerate, progressively greater amounts of random noise were added to a synthetic ultrasound waveform with a similar spectrum to that of in vivo ultrasound breast data acquired by CURE. The average absolute amplitudes of the random noise were, respectively, 0%, 20%, 40%, 60% and 80% of the maximum absolute amplitude of the synthetic ultrasound signal. The improved TOF picker according to the present invention can consistently detect the correct TOF in the presence of 80% white noise, which corresponds to a 4.5 dB SNR.

[0129] FIG. **11**A-**11**B and **12**A-**12** B illustrate signals and corresponding AIC values for both a high and low SNR ultrasound signal. In FIG. **11**A and **12**A are seen example signal representations with 0% and 80% random noise added, respectively. FIG. **11**B and **12**B indicate the value of AIC, from which a TOF can still be selected even at 80% noise added (SNR: 4.5 dB). The tests conducted herein, as well as work on preceding forms of AIC, such as the work of Kurz in [16] show that AIC-based TOF pickers can tolerate a relatively high noise level if an appropriate time window is used.

[0130] 10. Assessment of Inventive AIC Time-Of-Flight Picker.

[0131] To assess the performance of the improved AIC picker, TOF picks according to the present invention were compared with those produced through an amplitude threshold picker, and via manual picking; in this case of **1160** waveforms of in vivo ultrasound breast data acquired using the CURE device. Manual picking was conducted by recognizing the first rise time of the signal. To exploit the continuity of picked TOFs for adjacent waveforms [19], five consecutive waveforms were plotted on the computer monitor at the same time to further improve the accuracy of manual picking.

[0132] FIG. **13** is a snapshot image of the manual picking process, in which solid triangles indicate the manual TOF picks which were selected in response to clicking the computer mouse. To better illustrate ultrasound waveforms, the time windows were selected from 45 μs to 100 μs.

[0133] Since the amplitude threshold picker is much more sensitive noise, band-pass filtering was applied before picking the TOFs using an amplitude threshold. A second order zero-phase Butterworth band-pass filter with stop band corner frequencies at 0.3 MHz and 2.3 MHz, and pass band corner frequencies at 0.9 MHz and 1.7 MHz was used to filter the ultrasound breast data. To make a fair comparison, the same outlier removal procedures (median filtering and reciprocal pair check) were also applied to the amplitude threshold TOF picks.

[0134] FIG. **14**A-**14**B illustrate time difference data for 1160 in vivo ultrasound breast waveforms acquired using the CURE device (a ring transducer array). FIG. **14**A illustrates the absolute values of TOF differences between manual picks and amplitude threshold picks, while FIG. **14**B illustrates those TOF difference between manual picks and improved AIC picks according to the present invention. The statistics are given in Table 2 showing that for these 1160 in vivo ultrasound breast waveforms, over 85% of the TOFs picked by the inventive AIC picker are within three sample points (0.48 μs) from the manual picks. The mean value and standard deviation between the inventive TOF picker and manual picking are 0.4 μs and 0.29 μs, respectively. Among picks by the amplitude threshold picker, only 48% of them are within the three sample points from the manual picks, and the mean value and standard deviation from the manual picks are respectively 1.02 μs and 0.9 μs, which are much higher than those of the inventive TOF picking method.

[0135] Studies performed in association with this application utilizing other clinical ultrasound breast data indicate that the performances of our improved wavelet-AIC TOF picker and amplitude threshold-based TOF picker are comparable for data with high SNRs, but for data with high noise level (or low SNRs), the accuracy of the amplitude threshold picker drops abruptly. Moreover, for noisy ultrasound breast data, the failure rate of the amplitude threshold TOF picker is much higher than that of the improved wavelet-AIC TOF picker of the invention.

[0136] FIG. **9**A-**9**B illustrates two waveforms of different SNRs along with TOF picks by the above three methods. The type of TOF pick is shown in the figure based on best model ("○"), manual pick ("X"), and weighted average ("*") according to the present invention. It can be clearly seen that for the waveform in FIG. **9**A, which has a high SNR, the three TOF picks are consistent. The AIC pick according to the

invention is closer to the manual pick than is the best model (amplitude) pick, while in response to a noisy waveform, such as in FIG. **9**B, the amplitude threshold picker ("○") picked the wrong TOF, while the improved wavelet-AIC TOF pick according to the present invention remains comparable to the manual pick. The TOF picks in FIG. **9**A-**9**B are shown in Table 3.

[0137] FIG. **16** illustrates an example of overlays of the TOF picks by the inventive AIC TOF picker on the corresponding in vivo ultrasonic breast waveforms in which the solid dot on each waveform segment indicates the inventive AIC based TOF pick.

[0138] 11. Tomography Results of in vitro and in vivo Ultrasound Data.

[0139] TOF sound-speed tomography uses the TOF picks of ultrasound breast data for reconstruction. The tomogram quality depends directly on the quality and accuracy of TOF picks.

[0140] FIG. **17**A-C compares tomograms obtained using X-ray CT scans with ultrasonic imaging obtained for in vitro and in vivo ultrasound datasets using the inventive AIC TOF picks in comparison with amplitude threshold TOF picks. For this example all x and y axes span 200 mm in length. FIG. **17**A is a cross-section image from an X-ray CT scan of a breast which includes a phantom (tumor). The ultrasound sound-speed tomograms obtained using inventive AIC TOF picker is shown in FIG. **17**B, while the tomogram for using amplitude threshold TOF picks is shown in FIG. **17**C. It can be seen that the tomogram in FIG. **17**B contains significantly fewer artifacts than the tomogram in FIG. **17**C and much more closely resembles that of the X-ray CT scan. Moreover, the four inclusions and surrounding subcutaneous fat are better reconstructed in FIG. **17**B than those in FIG. **17**C. In contrast to in vivo ultrasound breast data, the phantom breast data has relatively low structure noise due to relatively simple internal structures.

[0141] FIG. **18**A-**18**B illustrate another comparison for in vivo ultrasound breast data acquired with the CURE device. For this example all x and y axes span 100 mm in length. The in vivo breast data used to obtain these images has a relative low SNR (~18 dB). The sound-speed tomogram produced using the inventive TOF picks, of FIG. **18**A, appears to have fewer straight-line artifacts compared to the one obtained using amplitude threshold TOF picks as shown in FIG. **18**B. For in vivo ultrasound breast data with relative high SNR (~25 dB), the difference between the corresponding sound-speed tomograms is minor, although the reconstruction with the inventive TOF picking still appears to be superior to the one produced using amplitude threshold TOF picks in terms of the mass detection and reconstruction noise. These comparisons again demonstrate that improved AIC TOF picking according to the present invention is much less sensitive to varying SNRs of ultrasound data than the amplitude threshold TOF picker.

[0142] 12. Section B: Conclusions.

[0143] This section has described an inventive automatic TOF picking method based on the Akaike Information Criterion (AIC) which has been successfully applied to in vivo ultrasound breast data, which for example has been collected using a ring transducer array. To improve the accuracy of the TOF picking, the improved picking method according to the invention incorporates all the information near the TOF point using a model inference method to determine the TOF of ultrasound signals. Further aspects of the invention utilize a median filter to remove TOF outliers. The resultant TOF picker of the invention can pick correct TOFs in noisy ultrasound data (with average absolute amplitudes of noise up to 80% of the maximum absolute amplitude of the signal) while the amplitude threshold based TOF picking method generally fails. For ultrasound breast data, the present inventive method is thus able to determine TOFs of a similar accuracy (quality) to those picked manually by an expert. One of the important advantages of the automatic TOF picker according to the invention is that it is operator independent, and is much less time-consuming than the manual picking. Accordingly, the present method makes it possible to incorporate automatic TOF picking within a clinical ultrasound tomography device without sacrificing outcome quality. It has been demonstrated that ultrasound sound-speed tomography using TOFs picked using the inventive automatic TOF picker method significantly improves the reconstruction accuracy and reduces image artifacts.

Section C

[0144] It should be appreciated that although the methods described were directed at ultrasonic breast tomography, these techniques can be implemented within any number of ultrasonic tissue imaging apparatus. The method is particularly well-suited for implementation on a system which receives ultrasonic waveforms and utilizes a computer for processing those signals. It should be appreciated, however, that the aspects of the invention can be implemented on any desired combination of software and hardware as will be recognized by one of ordinary skill in the art.

[0145] FIG. **20** illustrates an embodiment **50** of an ultrasonic imaging apparatus according to the present invention. A sensor head **52** is shown exemplifies as a ring configured for breast tomography, although it can be configured in any desired configuration for various forms of tissue testing. The sensor head **52** is configured with transmitters and receivers controlled by block **54**. All necessary data from the sensor head is conditioned as necessary in signal conditioning block **56**, from which data **58** on a plurality of ultrasonic signals is communicated to a computing device **60** containing at least one processing element **62** and memory **64**. Programming executable on computer **62** is configured for retention in memory **64**, and for executing the described method steps according to the present invention. The TOF picks can be utilized internal to the computer or be output **66** from the computer for use by image processing equipment **68** and image display and/or storage elements **70**. It will thus be appreciated that numerous medical ultrasonic devices can be configured according to the teachings of the present invention to improve resolution and quality of the ultrasonic information.

[0146] Although the description above contains many details, these should not be construed as limiting the scope of the invention but as merely providing illustrations of some of the presently preferred embodiments of this invention. Therefore, it will be appreciated that the scope of the present invention fully encompasses other embodiments which may become obvious to those skilled in the art, and that the scope of the present invention is accordingly to be limited by nothing other than the appended claims, in which reference to an element in the singular is not intended to mean "one and only one" unless explicitly so stated, but rather "one or more." All structural and functional equivalents to the elements of the above-described preferred embodiment that are known to

those of ordinary skill in the art are expressly incorporated herein by reference and are intended to be encompassed by the present claims. Moreover, it is not necessary for a device or method to address each and every problem sought to be solved by the present invention, for it to be encompassed by the present claims. Furthermore, no element, component, or method step in the present disclosure is intended to be dedicated to the public regardless of whether the element, component, or method step is explicitly recited in the claims. No claim element herein is to be construed under the provisions of 35 U.S.C. 112, sixth paragraph, unless the element is expressly recited using the phrase "means for."

[0147] 13. References for Section B.

[0148] [1] J. F. Greenleaf, A. Johnson, R. C. Bahn, and B. Rajagopalan, Quantitative cross-sectional imaging of ultrasound parameters, in Proc. IEEE Ultrason. Symp. (1977) 989-995.

[0149] [2] S. J. Norton and M. Linzer, Ultrasonic reflectivity tomography: reconstruction with circular transducer arrays, Ultrason. Imag 2 (1979) 154-184.

[0150] [3] P. L. Carson, C. R. Meyer, A. L. Scherzinger, and T. V. Oughton, Breast imaging in coronal planes with simultaneous pulse echo and transmission ultrasound, Science 214 (1981) 1141-1143.

[0151] [4] M. P. Andre, H. S. Janee, H. S., P. J. Martin, G. P. Otto, B. A. Spivey, and D. A. Palmer, High-speed data acquisition in a diffraction tomography system employing large-scale toroidal arrays, Int. J. Imaging Syst. and Technol. 8 (1997) 137-147.

[0152] [5] N. Duric, and P. Littrup, L. Poulo, A. Babkin, R. Pevzner, E. Holsapple, and O. Rama, Detection of Breast Cancer With Ultrasound Tomography: First Results with the Computerized Ultrasound Risk Evaluation (CURE) Prototype, Med. Phys. 34 (2007) 773-785.

[0153] [6] M. Baer and U. Kradolfer, An automatic phase picker for local and teleseismic events, Bull. Seism. Soc. Am. 77 (1987) 1437-1445.

[0154] [7] F. Boschetti, D. Dentith, and R. D. List, A fractal-based algorithm for detecting first-arrivals on seismic traces, Geophysics 61 (1996) 1095-1102.

[0155] [8] H. Zhang, C. Thurber, and C. Rowe, Automatic P-wave Arrival Detection and Picking with Multiscale Wavelet Analysis for Single-Component Recordings, Bull. Seism. Soc. Am. 93 (2003) 1904-1912.

[0156] [9] R. Ramananantoandro and N. Bernitsas, A Computer Algorithm for Automatic Picking of Refraction First-arrival-time, Geoexploration 24 (1987) 147-151.

[0157] [10] W. Su and A. M. Dziewonski, A. M., On the scale of mantle heterogeneity, Phys. Earth Planet. Interiors 74 (1992) 29-54.

[0158] [11] J. B. Molyneux and D. R. Schmitt, First-break timing: Arrival onset times by direct correlation, Geophys. 64 (1999) 1492-1501.

[0159] [12] S. Kullback and R. A. Leibler, On information and sufficiency, Annals of Mathematical Statistics 22 (1951) 79-86.

[0160] [13] D. R. Anderson, K. P. Burnham, and G. C. White, Kullbak-Leibler information in resolving natural resource conflicts when definitive data exist, Wildlife Society Bulletin 29 (2001) 1260-1270.

[0161] [14] R. Sleeman and T. van Eck, Robust automatic P-phase picking: an on-line implementation in the analysis of broadband seismogram recordings, Phys. Earth Planet. Interiors 113 (1999) pp. 265-275.

[0162] [15] N. Maeda, A method for reading and checking phase times in autoprocessing system of seismic wave data, Zisin. Journal of Seismological Society of Japan 38 (1985) 365-379.

[0163] [16] J. H. Kurz,, C. U. Grosse, and H. W. Reinhardt, Strategies for reliable automatic onset time picking of acoustic emissions and of ultrasound signals in concrete, Ultrasonics 43 (2005) 538-546.

[0164] [17] N. Duric, and P. Littrup, A. Babkin, D. Chambers, S. Azevedo, R. Pevzner, M. Tokarev, E. Holsapple, O. Rama, and R. Duncan, Development of ultrasound tomography for breast imaging: Technical assessment, Med. Phys. 32 (2005) 1375-1386.

[0165] [18] M. J. Mazerolle, Making sense out of Akaike's Information Criterion (AIC): its use and interpretation in model selection and inference from ecological data [Online]. Available: http://www.theses.ulaval.ca/2004/21842/apa.html.

[0166] [19] C. Li and R. L. Nowack, R. L, Seismic Tomography Using Travel-Time Surfaces for Experiments in the Laboratory, J. Geophys. Eng. 2 (2005) 231-237.

[0167] [20] R. Di Stefano, F. Aldersons, E. Kissling, and C. Chiarabba, Automatic seismic phase picking and consistent observation error assessment: application to the Italian seismicity, Geophys. J. Int. 165 (2006) 121-134.

[0168] [21] L. Birge and P. Massart, From model selection to adaptive estimation, in Festchrifft for L. Le Cam, D. Pollard Editor, Springer, New York, 55-88, 1997.

TABLE 1

TOF Picks for Different Conditions of FIG. 10A-10C

Condition	TOF (μS)
Raw data	100.80
Zero-Phase band-pass filtered data	100.16
Wavelet de-noised data	100.16

TABLE 2

Comparison of AIC and Amplitude Threshold Picks with Manual picks

	Mean Difference(μS)	Std. Dev. of Difference (μS)
Improved AIC picks	0.4	0.29
Amplitude threshold picks	1.02	0.9

TABLE 3

TOF picks by the Three Methods of FIG. 15A-15B

	FIG. 15A (μS)	FIG. 15B (μS)
Improved AIC picks	137.60	69.59
Manual picks	137.63	69.60
Amplitude threshold picks	138.16	72.07

What is claimed is:

1. A method of selecting time-of-flight (TOF) for ultrasound tomography waveforms generated by a given ultrasound tomography transmitter-receiver device directed on a tissue sample, comprising:

receiving a plurality of ultrasound waveforms from an ultrasound tomography transmitter-receiver device;

determining Akaike Information Criterion (AIC) values within a predetermined time window; and

selecting TOF for each said ultrasound waveform in response to the application of wavelet transforms searching said time window.

2. A method as recited in claim **1**, wherein said AIC is determined as a best-model in which the AIC value is minimized.

3. A method as recited in claim **1**:

wherein said AIC value is determined in response to multi-model averaging in which a weighted average of models is generated; and

wherein said weights for each model are assigned in response to the relative accuracy of each candidate model within the multiple models being considered.

4. A method as recited in claim **1**, wherein said predetermined time window comprises a timing window determined in response to transmitter-receiver geometry and the sound speed in water.

5. A method as recited in claim **1**, further comprising filtering to eliminate outliers in the TOF picks.

6. A method as recited in claim **5**, wherein said filtering comprises median filtering.

7. A method as recited in claim **5**, wherein said median filter has a length customized to the time differences between picked TOFs and the corresponding calculated TOFs in water based on the ring array geometry.

8. A method as recited in claim **7**, further comprising replacing filtered out values with median values.

9. A method as recited in claim **1**, further comprising comparing TOFs of reciprocal transmitter-receiver pairs and adjusting the associated TOF picks if they exceed a threshold.

10. A method as recited in claim **9**, wherein said threshold is selectable by a user based on individual requirements and data quality needs.

11. A method as recited in claim **9**, wherein said adjusting of TOF picks comprises replacing the TOF and its reciprocal TOF with an average of both TOF values.

12. A method as recited in claim **1**, wherein determining said AIC value comprises comparing AIC values to a series of models which are previously specified.

13. A method as recited in claim **1**:

wherein said AIC value is determined from, AIC(k)=k log (var(S(1,k)))+(N−k−1) log (var(S(k+1, N))), where S(1, k) and S(k+1, N) are the two segments in the selected time window; and

the variance function "var(.)" is determined from,

$$\mathrm{var}(S(i,\ j)) = \sigma^2_{j-i} = \frac{1}{j-i}\sum_{l=i}^{j}(S(l,\ l) - \overline{S})^2, \tag{2}$$

$$i \le j,\ i = 1, \ldots, N \text{ and } j = 1, \ldots, N$$

where $\overline{S}$ is the mean value of S(i,j).

14. A method as recited in claim **1**, further comprising generating ultrasound tomograph imaging in response to said TOF selections.

15. A method as recited in claim **1**, wherein said ultrasound tomograph comprises ultrasonic breast tomography.

16. A method as recited in claim **1**, wherein said method is configured to provide operator-independent, automatic, determination of TOFs for a set of ultrasonic signals.

17. A method as recited in claim **1**, wherein said method selects TOFs without necessitating manual picking of TOF timing points in each of said plurality of ultrasonic waveforms.

18. A method of selecting time-of-flight (TOF) for ultrasound tomography waveforms generated by a given ultrasound tomography transmitter-receiver device directed on a tissue sample, comprising:

receiving a plurality of ultrasound waveforms from an ultrasound tomography transmitter-receiver device;

determining a predetermined time window using the sound speed of water for the given transmitter-receiver device;

determining Akaike Information Criterion (AIC) values for the received data within said predetermined time window;

calculating a weighted average model for the signal segment;

selecting a TOF for each said ultrasound waveform in response to the application of wavelet transforms searching said time window;

applying a median filter to the TOF selections; and

correcting each TOF associated with said plurality of ultrasound waveforms in response to the difference between reciprocals.

19. An apparatus for processing for ultrasound tomography waveforms, comprising:

means for receiving a plurality of ultrasound waveforms from an ultrasound tomography transmitter-receiver device directed through a tissue sample;

a computer processor and memory coupled to said means;

programming executable on said processor for,

determining a predetermined time window,

determining Akaike Information Criterion (AIC) values within said predetermined time window, and

selecting TOF for each said ultrasound waveform in response to the application of wavelet transforms searching said time window.

20. A computer-readable media executable on a computer apparatus configured for processing ultrasound tomography waveforms, comprising:

a computer readable media containing programming executable on a computer processor configured for processing ultrasound tomography waveforms in response to receiving a plurality of ultrasound waveforms from an ultrasound tomography transmitter-receiver device directed through a tissue sample;

said programming executable on said processor configured for,

determining a predetermined time window,

determining Akaike Information Criterion (AIC) values within said predetermined time window, and

selecting TOF for each said ultrasound waveform in response to the application of wavelet transforms searching said time window.

* * * * *